100
12

A STUDY OF THE STRESSES AND DEFLECTIONS IN A RIGHT ANGLED JOINT BETWEEN TWO TUBES SUBJECTED TO PURE BENDING

A THESIS

Presented to

the Faculty of the Graduate Division

by

Harold Alfred Carless

In Partial Fulfillment

of the Requirements for the Degree

Master of Science in Aeronautical Engineering

Georgia Institute of Technology

June, 1959

"In presenting the dissertation as a partial fulfillment of the requirements for an advanced degree from the Georgia Institute of Technology, I agree that the Library of the Institution shall make it available for inspection and circulation in accordance with its regulations governing materials of this type. I agree that permission to copy from, or to publish from, this dissertation may be granted by the professor under whose direction it was written, or, in his absence, by the dean of the Graduate Division when such copying or publication is solely for scholarly purposes and does not involve potential financial gain. It is understood that any copying from, or publication of, this dissertation which involves potential financial gain will not be allowed without written permission.

A STUDY OF THE STRESSES AND DEFLECTIONS IN A RIGHT ANGLED JOINT BETWEEN TWO TUBES SUBJECTED TO PURE BENDING

APPROVED:

Date Approved by Chairman 29 May 1959

ACKNOWLEDGEMENTS

The author wishes to express his thanks for the assistance of the Lockheed Aircraft Corporation, Marietta, Georgia and, in particular, of Mr. D. G. Cumro, Structural Research Engineer, in making available the facilities for conducting the research work described in this thesis.

TABLE OF CONTENTS

LIST OF TABLES

LIST OF FIGURES

Figure | Page

NOTATION

c	distance of an element from the neutral axis of a beam in bending.
f	stress due to bending.
h	parameter used in the American Standard Code for Pressure Piping.
k	flexibility factor, the ratio of actual joint rotation to the calculated simple engineering theory rotation.
r	mean radius of the tube wall.
u	deflection of the tube wall radially outwards.
y	distance of an element in the tube wall from the center of the tube wall.
E	Young's Modulus.
I	moment of inertia of the tube cross-section.
M	applied bending moment.
R	radius of curvature of the center-line of a pipe bend.
α	half angle between adjacent mitre axes, reference the American Standard Code for Pressure Piping.
ϵ_1	strain in the circumferential direction.
ϵ_2	strain in the longitudinal direction.
ϵ_p	strain in the direction of a strain gage leg p.
σ_u, σ_v	principal strains.
λ	parameter defined on page 31.
μ	Poisson's Ratio.
θ	angle subtended between a radius and the tube in-plane diameter.

σ_p stress in the tube in the direction of strain gage leg p.

σ_u, σ_v principal stresses.

SUMMARY

An experimental investigation of the stresses and deflections in a right-angled joint between two tubes subjected to pure bending in the plane of the tubes is presented.

A comparison of this joint with the circular pipe bend suggests that the deflections and internal stresses will be similar. The changes in direction of the tension and compression forces in the tubes caused by the bending cause inward components of force which ovalize the tube cross-section near the joint. This ovalization causes circumferential bending stresses in the walls of the tube, which will be a maximum close to the joint. Similarly, the internal energy in the tubes is increased by the ovalization. Thus the joint is more flexible than simple engineering theory would predict.

Two Plexiglas joints were constructed of six inch diameter tubing. Measurements of the flexibility of the joints and of the tube diameter changes due to the application of pure bending were made. Strain measurements were made using electrical resistance strain gages and Stresscoat.

Local ovalization of the tubes was measured near the joint. This ovalization decreased approximately

exponentially as distance from the joint increased.

The flexibility of the joints is compared to that calculated from simple engineering theory to obtain values of the "Flexibility Factor". This Factor is compared with factors given in the American Standard Code for Pressure Piping for similar pipe bends and mitred joints. The Factor for the thinner-walled specimen was considerably greater than the value given in the Code for a similar pipe bend or mitred joint.

Strain data show that a local region of high stress is present on the centroidal axes of the tubes near the joint. The direction of this stress is approximately parallel to the joint. The magnitude is such that early fatigue failures can be predicted under repeated loading conditions, particularly if there are any stress-raisers present in this region.

CHAPTER I

INTRODUCTION

It has been known for many years that the stresses existing in a pipe bend subjected to bending loads are more complicated than simple engineering theory would predict, and that the deflections due to imposed bending are many times greater than would be predicted by the simple engineering bending formula. Original work on this subject was published by Theodore von Kármán in 1911 (1). This subject has been of sufficient importance to designers of piping systems that considerable research has been devoted to this subject. Reference (2) gives an extensive list of references on the subject. Industrial requirements for the design of pipe bends are established by the American Society of Mechanical Engineers (3), and give formulae for the "Flexibility Factor", "Stress Intensification Factor", and "Flexibility Characteristic" for bends or joints in piping.

In the design of landing gear for airplanes, it is not uncommon to find a similar joint existent at the intersection of the axle and the vertical leg of the gear. Both of these members are usually hollow steel tubes of more or less complicated shape and may be of integral

construction, but are more likely to be formed by joining two separate tubes together by flash welding. The joint so formed cannot be described as a pipe bend, and the formulae developed for the pipe bend are not applicable. In order to design such a joint with the minimum of weight, it is necessary to develop a theory for this more complicated problem.

This study investigates the conditions prevailing in a 90-degree joint in a hollow pipe, formed by cutting the two parts at 45 degrees and welding or otherwise fusing them together (Fig.1). The method of loading investigated is a pure bending in the plane of the joint. The stresses existent in such a joint are investigated, and the stiffness of the joint is compared to that which would be predicted by simple engineering theory. An extensive literature search has not revealed any previous investigation of this problem, either theoretical or experimental.

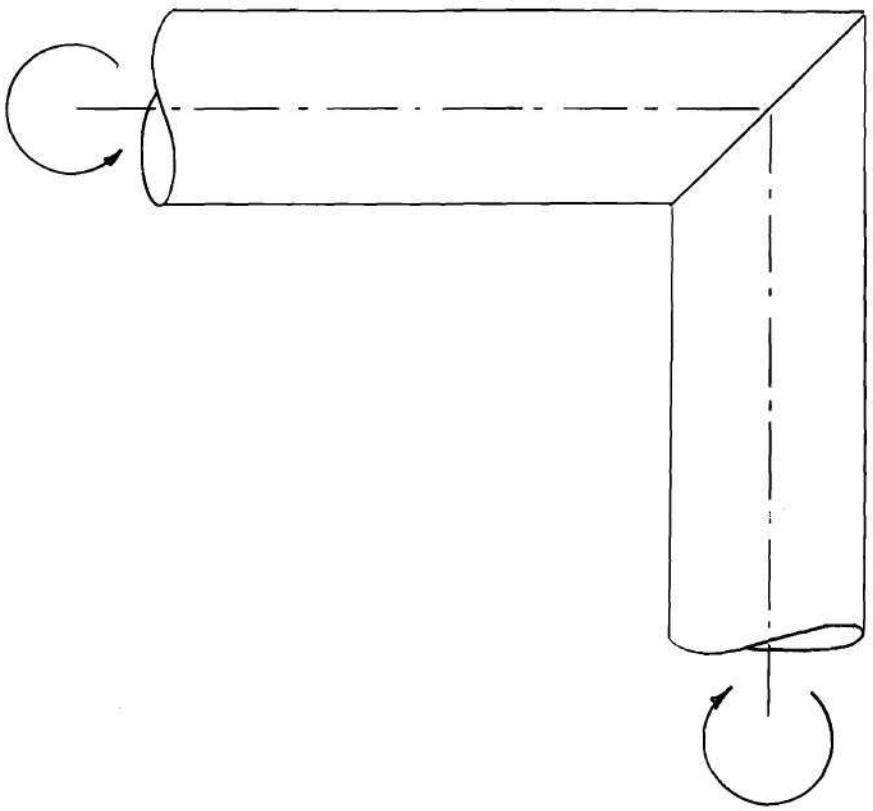

Fig. 1. In-Plane Bending of a 90-degree Joint in a Thin-Walled Tube.

CHAPTER II

COMPARISON WITH THE PIPE BEND

The analysis of the pipe bend subjected to a bending moment in its own plane, originally investigated by von Kármán (1), is presented by Den Hartog in (4). Simple engineering theory predicts that tension and compression forces will be developed in the fibers of the pipe. However, due to the curvature, both the fibers in tension and the fibers in compression develop radial components of force which tend to cause flattening or ovalization of the tube cross-section (Fig. 2). This flattening diminishes the energy stored in the tube due to the longitudinal forces, but causes increased energy due to the distortion of the cross-section. The pipe bend is analyzed by von Kármán by using the Principle of Least Work to determine the distortion of the tube and the internal stresses.

Examination of the joint under investigation, shown in Fig. 3, suggests that at a large distance from the joint the stresses will be given by the simple engineering formula

$$f = \frac{Mc}{I} .$$

If these stresses existed unchanged at the joint, then the forces at the joint would combine to give resultant forces

at 45 degrees to the axes of the two tubes (Fig. 3). These forces would clearly cause flattening of the tubes, which would be a maximum close to the joint.

The distortion of the tubes in the neighborhood of the 90-degree joint is therefore expected to be similar to that in the pipe bend. Distortion of the tube cross-section will cause circumferential bending stresses in the walls of the tube. It is also expected that, similar to the pipe bend, such a joint will be more flexible than simple engineering theory would predict.

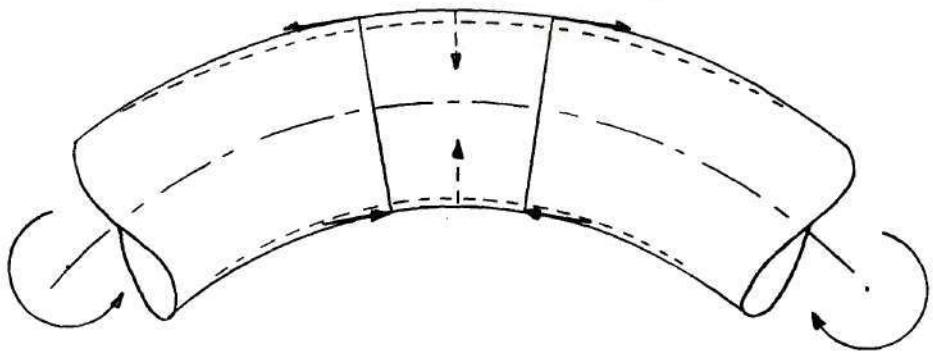

Fig. 2. Distortion of Pipe Bend caused by Bending.

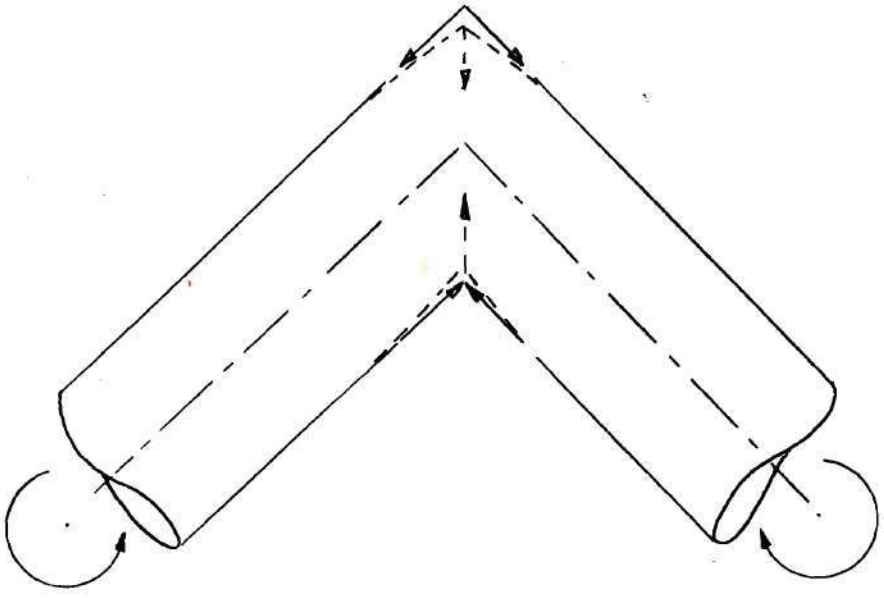

Fig. 3. Analogous Distortion of Tube Joint.

CHAPTER III

EXPERIMENTAL INVESTIGATION

Test Specimens.--Two model joints were constructed of Plexiglas tubing with nominal dimensions as follows:

Specimen 1 - 5.844 inches inside diameter
0.125 inches wall thickness

Specimen 2 - 5.594 inches inside diameter
0.250 inches wall thickness

Plexiglas tubing was chosen for constructing the models for the following reasons:

(a) Material was readily available at a reasonable cost.
(b) The joint could be fabricated readily by a simple gluing procedure.
(c) Plexiglas has a low modulus of elasticity, and hence only small forces would be required to bend the models.
(d) Use of a transparent material facilitated the installation of strain gages on the inside surface of the model because the critical area was visible through the wall of the tube.

The two tubes were cut at 45 degrees on a band saw and the

cut surfaces were sanded as flat as possible on a disc sander with a fine grit. The two halves of each specimen were then placed together in a light holding jig and cemented together.

Initially ethylene dichloride was used to bond the two halves of the specimens together. This is a solvent for Plexiglas but has no filling properties. First bonds made in this manner were poor and an attempt was made to improve the joints by injecting into the void spaces Plexiglas Cement PS 18 manufactured by the Rohm and Haas Company mixed with Cadox B.C. Cadet Catalyst. After the joints had dried for several days, experiments were begun. However, both specimens failed in the joint after very little loading, and Specimen 2 was damaged beyond repair.

Specimen 1 was resanded and glued together again using Plexiglas Cement PS 18 and the Catalyst. The plastic mixture was applied to the surfaces of both halves of the joint, and the two parts were pressed together in the holding jig, allowing excess cement to be forced out of the joint. After drying for several days with a hot air dryer, additional cement was brushed around the outside and inside of the joint to build up the local thickness and reinforce the joint further. The joint was then allowed to cure for several additional days before loading. This specimen was used for the remainder of the test program.

Test Jig.--A simple test jig, shown in Figs. 4 and 5, was built to hold one end of the specimen and to apply a pure bending moment to the other end. The bending was applied by equal cable loads pulling in opposite directions, spaced at a distance of 6 1/8 inches apart.

Initially loads were applied through a calibrated hydraulic jack. However, difficulties were experienced in repeating measurements accurately due to jack friction at the small pressures being used, and in loss of load due to small oil leaks in the jack and hand pump. The jig was, therefore, changed to strain the specimen by a turnbuckle and measure the loads with a calibrated transducer in one of the cables. Transducer strains were measured with a Baldwin L-indicator. Loading by this method gave much better repeatability of readings, and had the advantage that the strains in the specimen remained effectively constant, even though the transducer indicated a reduction in load due to creep in the specimen after loading was held for a long time.

Specimen Deflections.--Deflections of the center-line of the specimens were measured with a cathetometer (traveling microscope) sighting on targets marked on paper flags glued to the specimens (Fig. 6). Measurements were made in X and Y coordinates at several load levels, and were found to be repeatable to approximately $\pm$0.001 inches. Readings are

given in Tables 1 and 2, and a typical deflection curve is plotted in Fig. 7.

An attempt was made to measure the flattening of the specimen in the loading plane by measuring X and Y coordinates of points on the tube profile as seen by the cathetometer. However, these figures proved to be erratic, and are not presented.

Measurements of tube diameters, both in plane and out of plane, were made at several load levels with micrometers reading to 0.001 inches. These measurements were made at intervals along each tube. Readings are given in Tables 3 and 4, and are plotted in Figs. 14 through 18. Some scatter was evident in the readings from the micrometers owing to difficulty in obtaining a consistent pressure on the micrometer screw, and also due to local variations in tube dimensions. Readings indicated a local distortion in the region of the loading cables, and these figures are not presented in the Tables.

Strain Gage Readings.--Electrical resistance strain gages were glued to the inside and outside surfaces of the upper arm of Specimen 1 as shown in Fig. 8. These gages were placed on the major and minor axes of the tube where it was anticipated that circumferential stresses due to tube distortion would be maximum. Gages on the side of the tube were arranged

in 45-degree rosette patterns to enable the full strain patterns to be determined. On the upper and lower surfaces of the tube, gages were located in longitudinal and transverse directions only, as the symmetry of the specimen suggested that no shear stresses would be present in these areas. Gages were installed with Duco household cement. Details of gages used are given in Table 5. Gages were read with a Baldwin L-indicator using a 20-channel switching and balancing box. Readings are given in Table 6, and are evaluated in Table 7.

Stresscoat Analysis.--At the end of the test sequence a Stresscoat investigation of Specimen 1 was conducted (5). This was delayed until the end of the program because it was thought that the Stresscoat solvent might cause crazing of the surface of the Plexiglas. However, no evidence of this was noted during the test. The specimen was sprayed with aluminum-pigmented undercoating lacquer ST-840 and allowed to dry for 15 minutes. It was then sprayed with Stresscoat 1206. At the same time calibration strips were similarly sprayed. The specimen and calibrating strips were allowed to dry overnight.

Loading was conducted on the following morning, when it was found that the Stresscoat sensitivity was 1200 micro-inches per inch. Load was applied to the specimen in

increments of 25 pounds of cable load up to a maximum of 100 pounds. Between each loading the specimen was unloaded and allowed to rest for approximately ten minutes. At each load the Stresscoat was examined closely and the boundaries of the cracked area marked with a wax pencil and also the directions of the cracks. The pattern obtained is shown in Figs. 9 and 19.

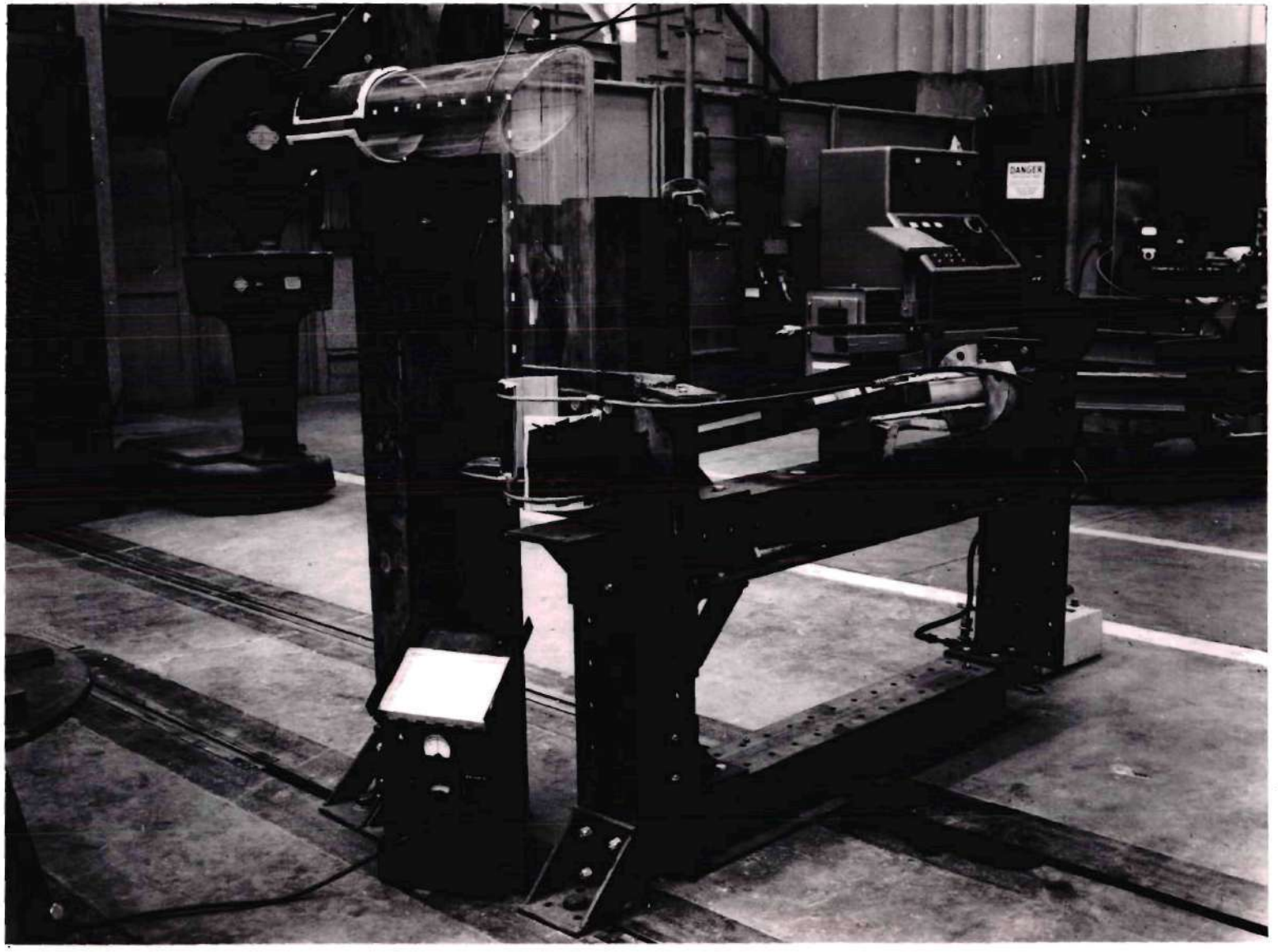

Fig. 4. Test Jig

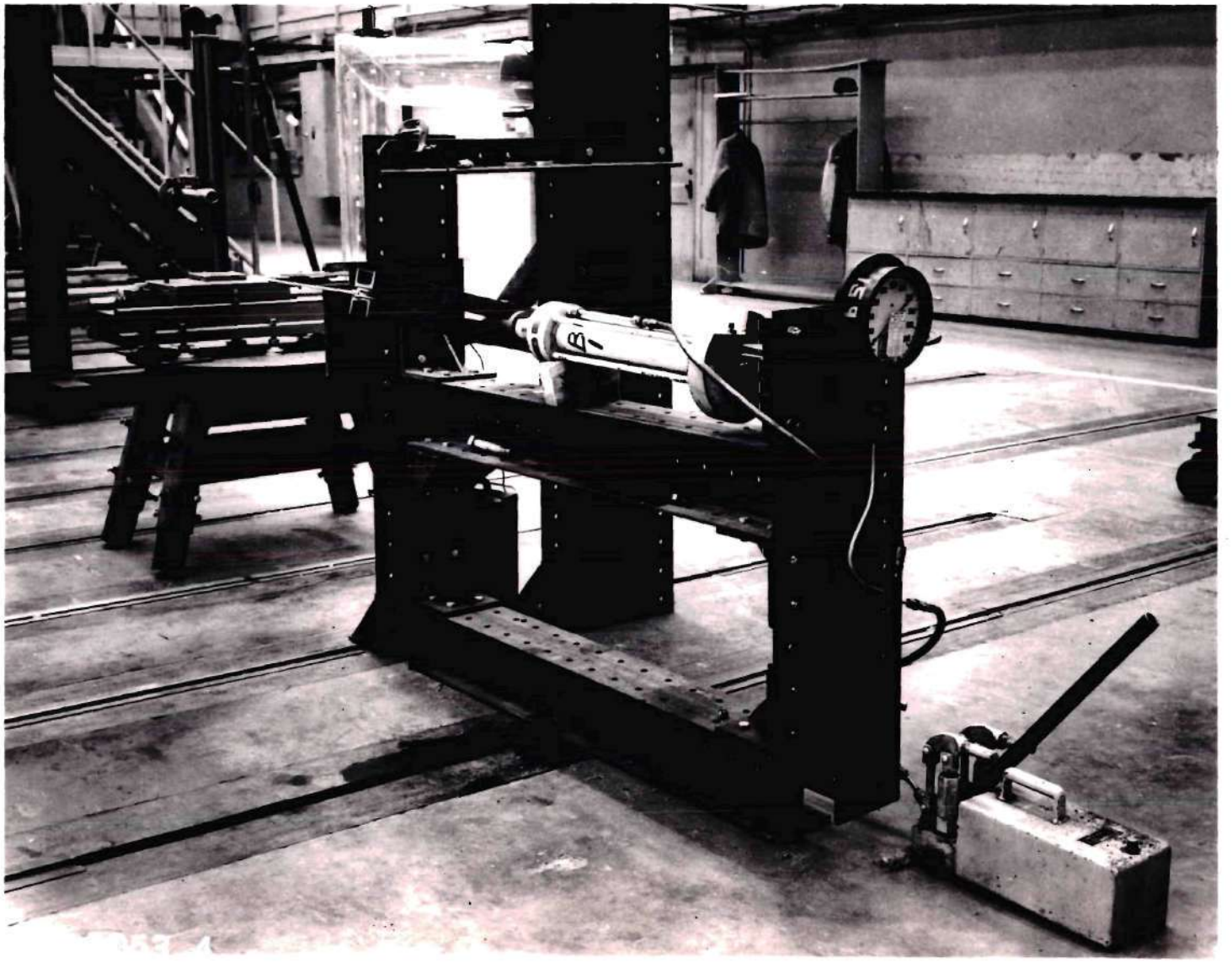

Fig. 5. Test Jig

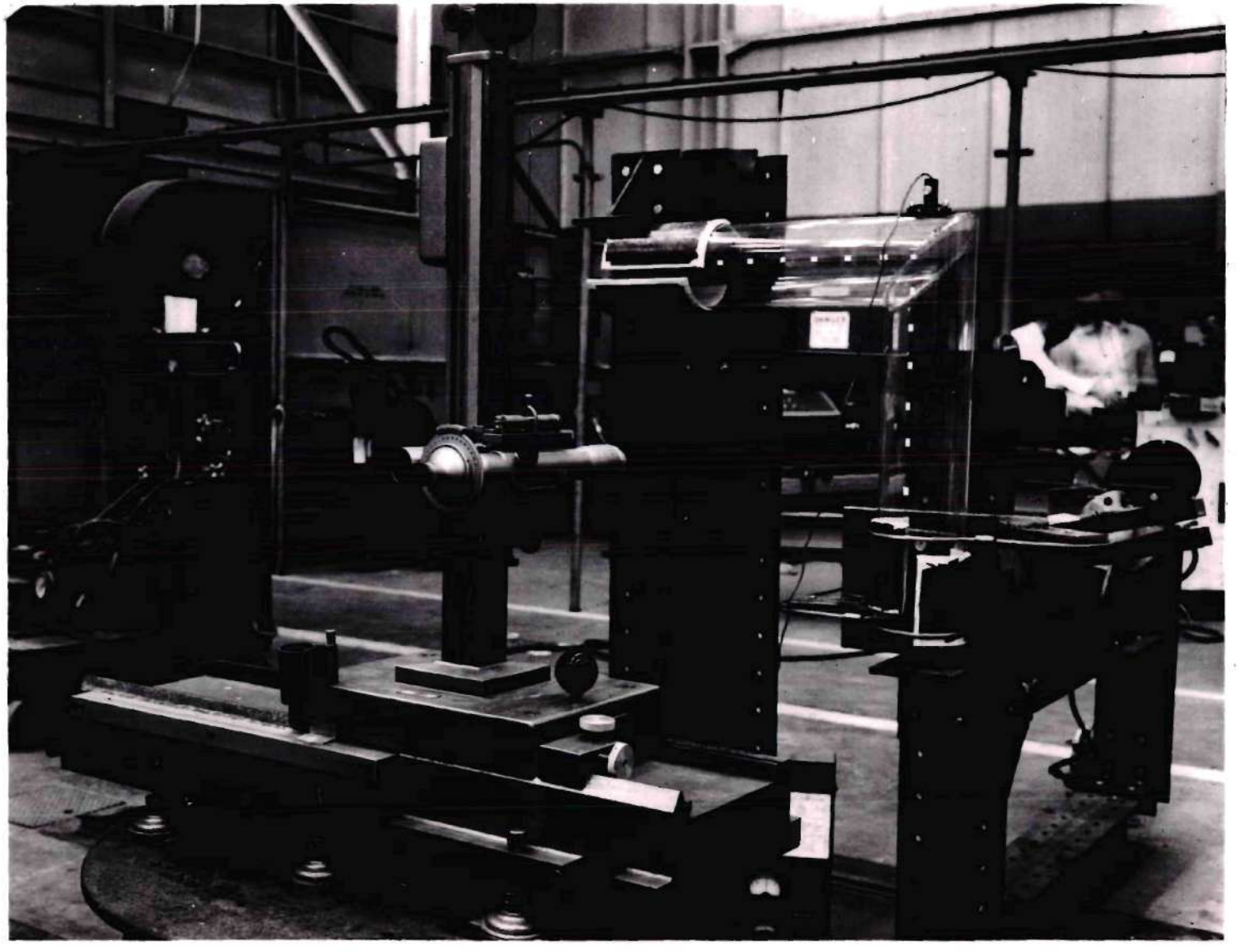

Fig. 6. Cathetometer set up for reading deflections

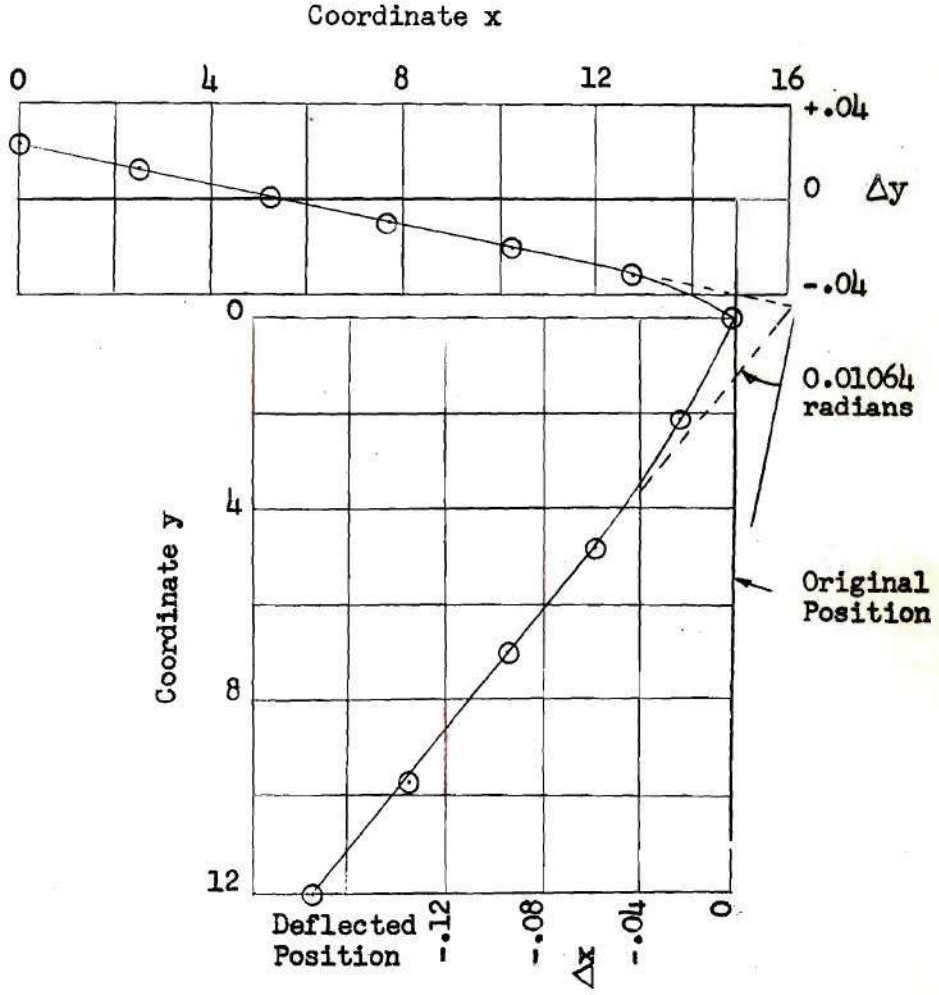

Fig. 7. Deflection of Specimen 1.

Moment 416 inch - pounds.

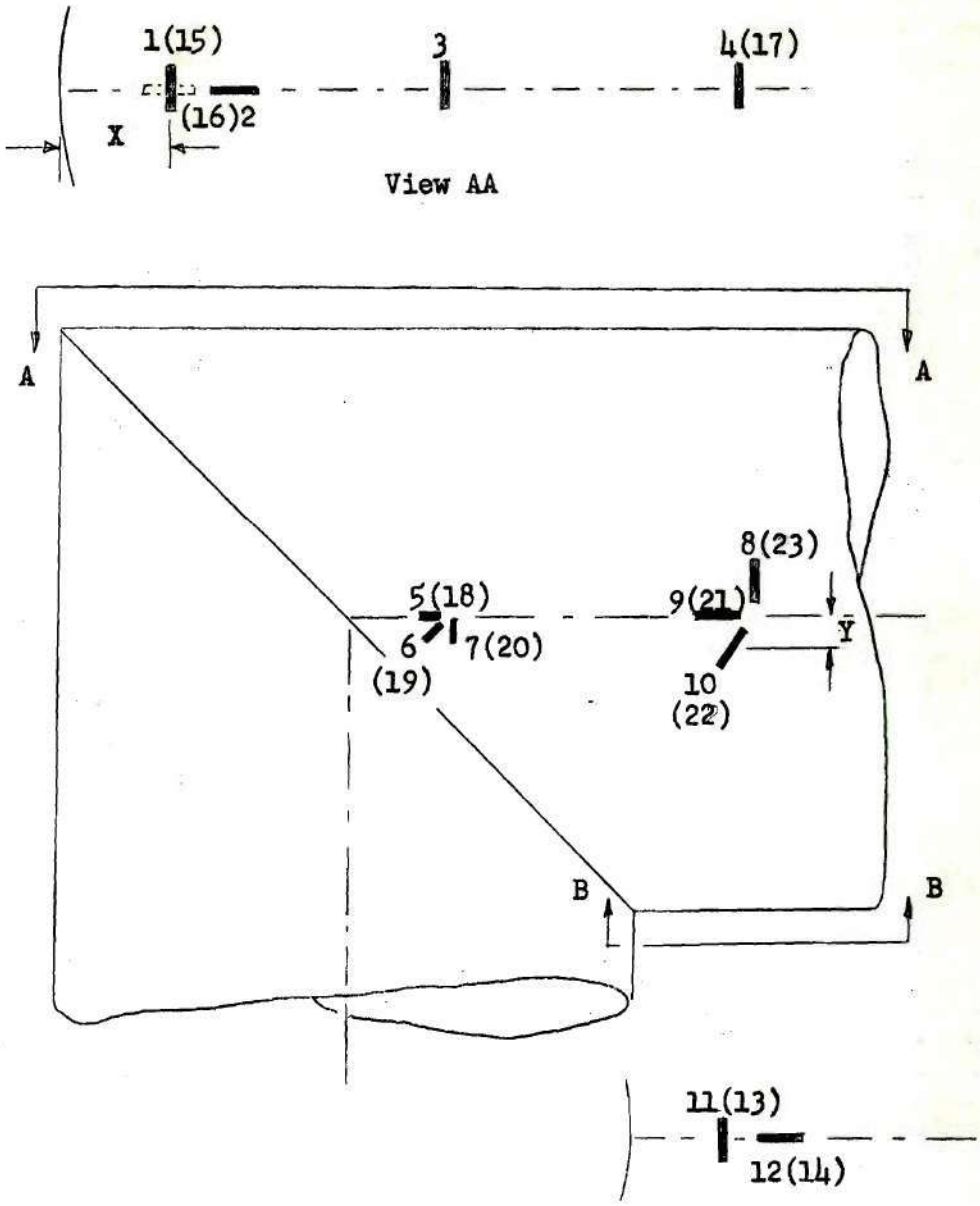

(Numbers in parentheses denote internal gages)

Fig. 8. Location of Strain Gages.

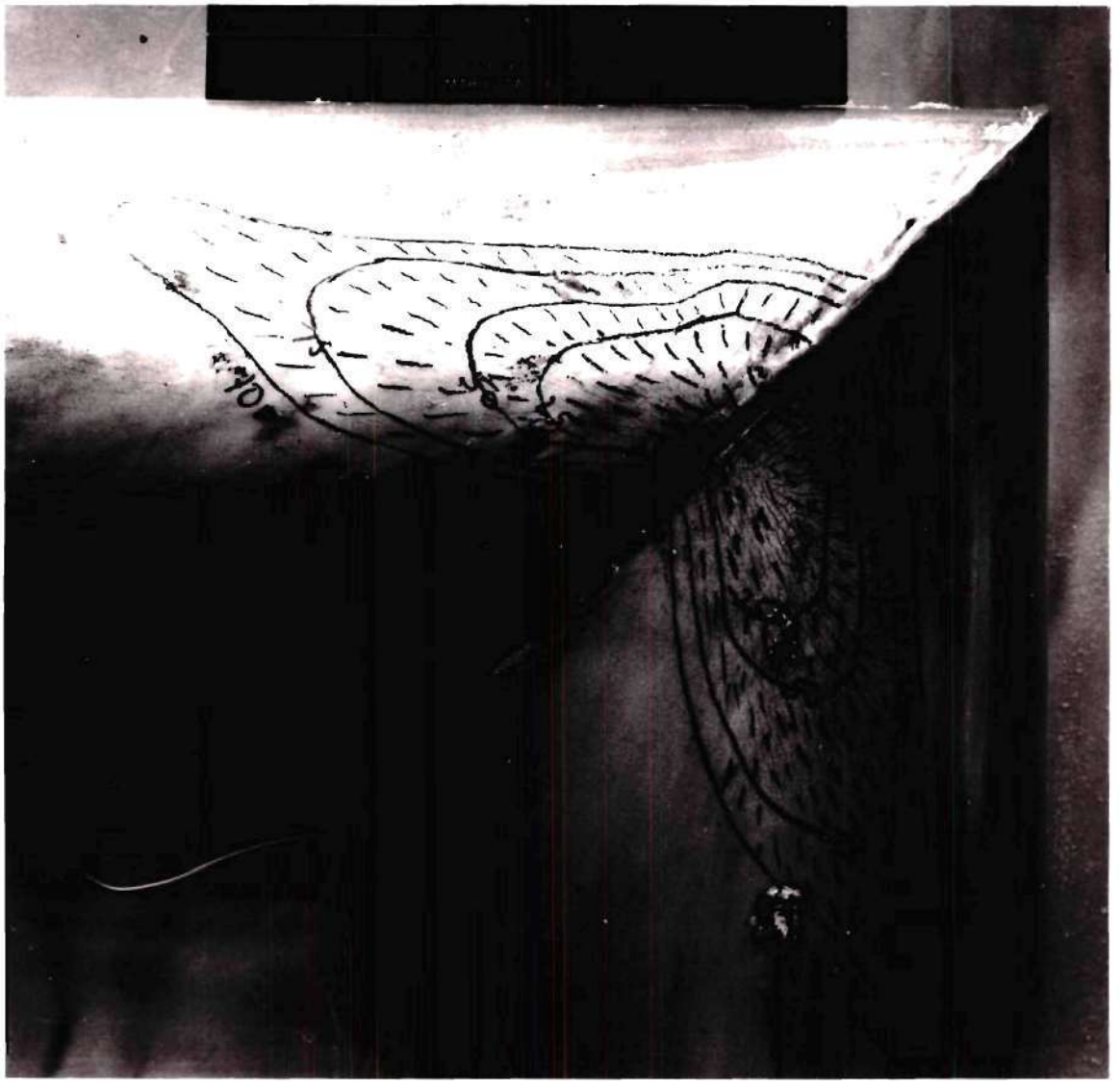

Fig. 9. Stresscoat pattern

CHAPTER IV

ANALYSIS OF TEST RESULTS

Joint Stiffness

Specimen 1:

$I = 10.446 \text{ in}^4$ $\qquad \frac{t}{r} = \frac{0.125}{2.985} = 0.0419$

$E = 400{,}000 \text{ lb/in}^2$ (6)

For moment of 1,000 inch-pounds, radius of curvature expected (simple engineering theory)

$$= \frac{EI}{M} = \frac{400{,}000 \times 10.446}{1{,}000} = 4180 \text{ in.}$$

Expected change in slope through the joint, taking an effective tube length of $\frac{\pi r}{2}$ as in the American Standard Code for the 90-degree single-mitred joint (3)

$$= \frac{\pi \times 2.985}{2 \times 4180} = 0.001122 \text{ radians.}$$

Fig. 13 shows the angular changes obtained on Specimen 1, and the best straight line is drawn to represent all points. From Fig. 13, experimental angle change obtained for 1,000 inch-pounds is 0.04 radians. Hence ratio of deflections

$$\frac{\text{Experimental}}{\text{Expected}} = \frac{0.04}{0.001122} = 35.7$$

Measurements hence show that the joint is 35.7 times as

flexible as simple engineering theory would predict over the length of tube considered.

On the plots of deflection, curvature of the center-lines of the specimens could not be distinguished except locally near the joint. Elsewhere, the deflections plotted as straight lines. The greater curvature obtained near the joint was very clear on these plots (Fig. 7).

Specimen 2:

$I = 19.60 \text{ in}^4$ $\qquad \frac{t}{r} = \frac{0.250}{2.922} = 0.0856$

$E = 400{,}000 \text{ lb/in}^2$

Expected radius of curvature (simple engineering theory)

$$= \frac{EI}{M} = \frac{400{,}000 \times 19.60}{1{,}000} = 7840 \text{ in.}$$

Expected change in slope through the joint with effective tube length of $\frac{\pi r}{2}$

$$= \frac{\pi \times 2.922}{2 \times 7840} = 0.000584 \text{ radians.}$$

From Fig. 13, experimental angle change obtained for moment of 1,000 inch-pounds was 0.00556 radians. Hence ratio of deflections

$$\frac{\text{Experimental}}{\text{Expected}} = \frac{0.00556}{0.000584} = 9.52$$

These results confirm the expected result that the smaller

the ratio $\frac{t}{r}$ the more flattening will be caused by the bending, and the greater will be the ratio of actual deflection to the calculated simple engineering theory deflection. These two ratios are shown in Fig. 12.

Tube Diameter Changes

Specimen 1.--Diameter changes were measured for applied moments of 416 and 612 inch-pounds. Measured changes along both major diameters, decreases in the case of the in-plane diameters, and increases in the case of out-of-plane diameters, are shown in Figs. 14 and 15. Fig. 10 shows both these curves replotted for unit applied moment. It will be noted that the two curves agree very closely.

Specimen 2.--A similar procedure was followed for three sets of readings shown in Figs. 16, 17 and 18. These have been replotted in Fig. 11 for unit applied moment. Reasonable agreement is shown, and the average of all three sets is also shown.

A comparison of the tube diameter changes for the two specimens at three distances from the external corner of the joint is given below at a common applied moment of 1,000 inch-pounds.

Distance in.	Specimen 1 in.	Specimen 2 in.	Ratio
5.0	0.226	0.0397	5.7
10.0	0.122	0.0165	7.4
15.0	0.066	0.0051	12.9
Average	-	-	8.7

Strain Gage Results

From the limited amount of data available from the strain gage results on Specimen 1, presented in Tables 6 and 7, it is seen that the strains followed the pattern expected.

For lateral strains, gages 1, 3 and 4 on the upper surface outside read negative strain. Gage 17 on the upper surface inside read positive strain. Gage 11 on the lower surface outside read negative strain. Gage 13 on the lower surface inside read positive strain. Gages 7 and 8 on the side of the tube on the outside read positive strain. Gages 20 and 23 on the side on the inside read negative strain. All these are consistent with the type of tube ovalization expected.

For longitudinal strains, gage 2 on the upper surface read a low positive strain. Gages 12 and 14 on the lower surface read a low negative strain. These are consistent with the applied bending. However, the rosette gages on the sides of the tube yielded some surprising results. These gages

were located on the neutral axis of the tube. It was therefore expected that little or no longitudinal strain would be present. Since no shear load was applied to the tube, it was expected that no shear stresses would be present, and that therefore these gages would indicate only a circumferential strain due to the tube ovalization. These gages, however, indicated considerable longitudinal strain. Also the circumferential strains in the gages close to the joint were much higher than in any other location.

Principal strains and stresses determined from these rosette readings are shown in Table 7. Comparing these for rosettes (5,6,7) and (18,19,20), and for rosettes (8,10,9) and (21,22,23), which were approximately back to back with each other, it will be seen that the measured principal strain directions were in close agreement. The rosette gages close to the joint showed extremely high strains in directions roughly parallel to the joint surface.

The readings of longitudinal gages 1, 3 and 4 were as follows:

Gage 1 - 1.15 in. from the corner of the joint - 491 x 10^{-6}
Gage 3 - 4.0 in. " " " " " " - 828 x 10^{-6}
Gage 4 - 7.1 in. " " " " " " - 1323 x 10^{-6}

These figures suggest the possibility that the local distortion of the wall of the tube on the upper surface

caused by the ovalization decreases to zero at the corner. Since it also decreases to zero at a large distance from the joint, this suggests that there is some place, probably close to Gage 4, where the distortion is at a maximum. An attempt was made to check this by measuring the change in profile of the tube under load with the cathetometer. However, no trace of such a distortion could be detected in the readings.

Stresscoat Results

Fig. 19 shows the boundaries of the cracked areas in the Stresscoat, and also the crack directions. The boundaries indicate the limits of the regions on the tube outer surface where the strain was equal to or greater than 1200 micro-inches per inch for the four different load levels. The crack directions are perpendicular to the principal tension stress directions in the Plexiglas. Interpreted in a different way, the boundaries enclose the areas where the strains are respectively greater than 4800, 3600, 2400, and 1200 micro-inches per inch for an applied moment of 612.5 inch-pounds.

Strains obtained from the Stresscoat are compared with the principal strains from the strain gages in Fig. 19. The patterns confirm the strain gage indication that the region of highest strain on the outer surface is near the joint, approximately on the centroidal axis, and that the

strain direction here is parallel to the joint. Further away from the joint, the principal strain directions are approximately in the circumferential direction. It will be noted, however, that the cracked area moves away from the centroidal axis of the tube away from the joint, indicating that the stress distribution within the tube is more complex than was indicated in Chapter II.

Comparison of Deflection and Strain Gage Readings (Specimen 1)

From Fig. 10 the measured ovalization of the tube at 7.1 inches from the outside corner of the joint was 0.1052 inches for a moment of 612.5 inch-pounds.

Den Hartog (4) gives the following formula for the circumferential strain:

$$\epsilon_1 = - \frac{3u \cos 2\theta}{r^2} \cdot y$$

where u is the radial deflection outwards of the tube at the end of the in-plane diameter. ($\theta = 0$)

r is the mean radius of the tube wall.

y is the distance of the element in the tube wall from the center of the tube wall.

θ is the angle between a radius and the tube in-plane diameter.

Hence the predicted strain on the surface of the tube at the end of the in-plane diameter is

$$= - \frac{3}{2.979^2} \times 0.0526 \times 0.0625 \times 10^6$$

$$= - 1110 \text{ micro-inches per inch.}$$

Measured strains round this section of the tube were as follows:

At $\theta = 0$ outer surface = -1323
inner surface = +1358
$\theta = 90^\circ$ outer surface = +2015
inner surface = -1447
$\theta = 180^\circ$ outer surface = -904
inner surface = +689

It will be seen that there is an approximate correlation between these strains and those calculated from the measured diametral change at this section. However, it is clear that the true strain pattern in the tube is more complex than the above formula assumes.

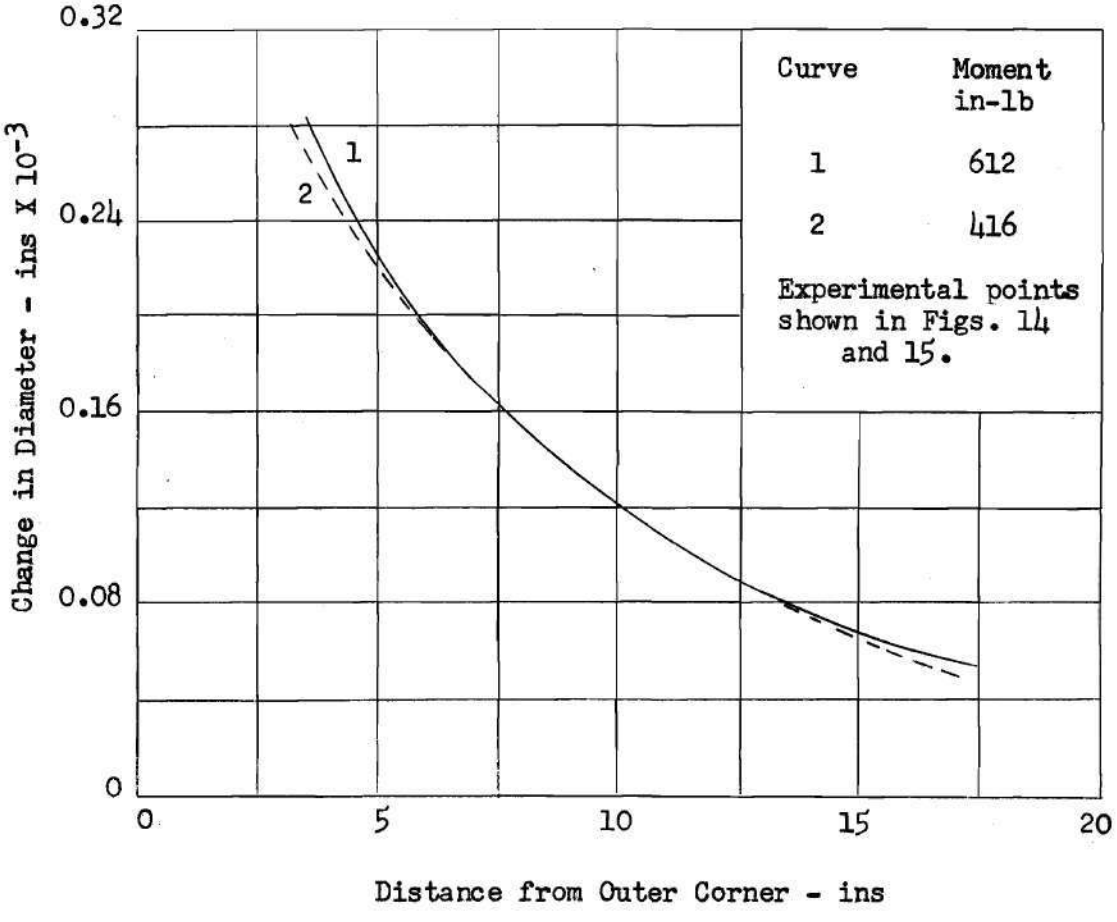

Fig. 10. Specimen 1. Measured Changes in Diameter for Unit Moment.

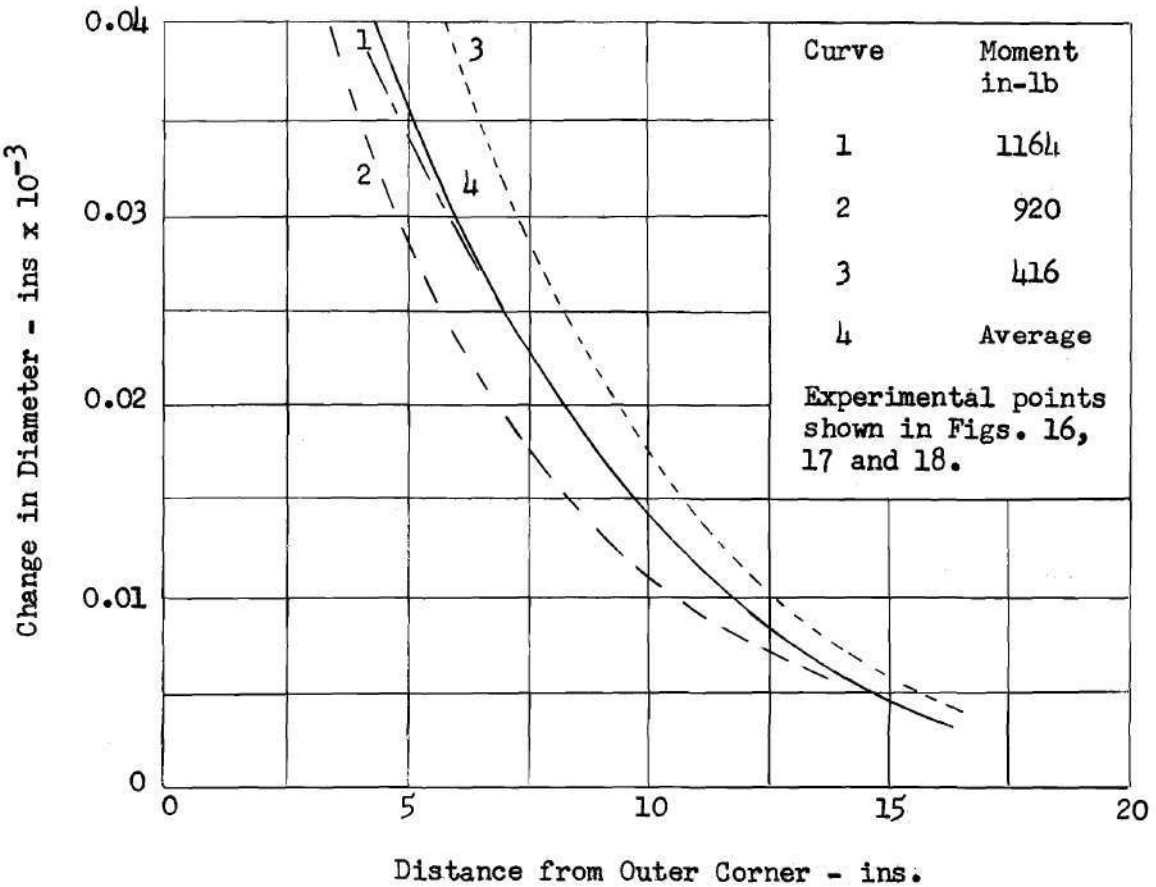

Fig. 11. Specimen 2. Measured Changes in Diameter for Unit Moment.

CHAPTER V

DISCUSSION AND COMPARISON OF TEST RESULTS WITH PUBLISHED DATA

Joint Deflections.--Test results confirm that a right-angled joint in a thin-walled tube is many times more flexible than simple engineering theory would predict. Fig. 12 shows the correlation between $\frac{t}{r}$ and the Flexibility Factor k.

The American Standard Code for Pressure Piping (3) gives the following formula for the Flexibility Factor k for a single mitred bend in a pipe:

$$k = \frac{1.52}{h^{5/6}} \quad \text{where} \quad h = 1 + \frac{\cot \alpha}{2} \frac{t}{r}$$

α = half angle between adjacent mitre axes.

Substituting $\alpha = 45^{\circ}$ these formulae become:

$$h = \frac{t}{r} \qquad k = 1.52 \left(\frac{t}{r}\right)^{-5/6}$$

The following values of k are obtained:

$\frac{t}{r}$	k
0.025	32.9
0.05	18.4
0.075	13.1
0.10	10.3
0.20	5.8

In the case of a pipe bend the Standard gives:

$$k = \frac{1.65}{h} \qquad \text{where } h = \frac{tR}{r^2}$$

and R = radius of the bend.

For R = 2r this gives $h = \frac{2t}{r}$ and the following values of k:

$\frac{t}{r}$	h	k
0.025	0.05	33.0
0.05	0.10	16.5
0.075	0.15	11.0
0.10	0.20	8.25

The American Standard Code values for the Flexibility Factor k for the single mitre bend, and for the circular pipe bend with R = 2r are compared with the experimental values obtained for the two Plexiglas tubular joints in Fig. 12. It will be observed that the experimental value of k obtained from Specimen 1 is much higher than the values obtained from the Code. Markl states (7):

> In the absence of a theoretical development, the sparse available data on mitre bends . . . have been evaluated conservatively in the proposed rules as
>
> $$k = \frac{1.52}{h^{5/6}} \qquad \text{where } h = \frac{tR}{r^2}$$

It will be noted that this statement does not agree with the American Standard Code for the mitre joint.

Rodabaugh and George (8) also give curves relating the factor k with a parameter λ for long radius elbows with $\frac{R}{r} = 3$, where $\lambda = \frac{tR}{r^2(1-\mu^2)}$. For an elbow of the dimensions of Specimen 1, with $\frac{R}{r} = 3$

$$\lambda = \frac{0.125 \times 3}{2.984 \times 0.8775} = 0.143$$

For this value of λ Rodabaugh and George give k = 12.5 for the elbow, as compared with k = 35.7 measured in the Plexiglas specimen. The curves given in this reference are for steel piping. However, they should be applicable to any material, provided that the elastic limit of the material is not exceeded. Since the shape of the 90-degree mitred bend is radically different from that of the elbow, a close correlation of flexibility factors cannot be expected.

Tube Ovalization.--Ovalization of the tubes was measured in the joint region. This decreased approximately exponentially away from the joint. Within the limits of accuracy of the measuring equipment used, the decrease of the in-plane diameters was equal to the increase of the out-of-plane diameters.

Some experimental data on the diametral changes observed in a 4½ inch diameter x 0.095 inch wall pipe, bent to a radius of six inches, is given by Markl (9). Measured diametral changes in the bend are plotted to an undefined

scale. These plots show maximum ovalization at the center of the bend, decreasing approximately exponentially in the straight pipe welded to the end of the bend. It is stated that "flattening, of the order of ten per cent of the maximum observed, was evident in the tangents over 1½ diameters away from the welded joint." This figure compares reasonably well with the experimental deflections shown in Figs. 10 and 11.

Strain Data.--Both strain gage and Stresscoat data indicated that a localized area of high strain exists near the joint on the centroidal axes of the tubes. This strain was greatest on the inside surface, and indicated a tube wall bending about an axis approximately normal to the joint. Gross (10) makes the following statement:

> The data establish for the first time that the largest stress in a pipe bend occurred on the inside surface, it was a stress in the transverse direction, and at a point where from similarity with curved bars the stress-free axis was assumed to be.

Markl (11) in discussing fatigue failures of mitred joints says:

> From the study of the failed specimens presented earlier, it is apparent that mitred joints at best behave like bends of very sharp curvature, but that usually the local stresses introduced by the sudden directional change overshadow this effect and lead to even earlier failure.

Pardue and Vigness (12) state:

> A bending moment decreasing the bend radius causes a transverse compressive stress which is a maximum at the neutral plane. This stress always adds to the local transverse stress on the inside wall of the tube, and subtracts from the local stress on the outside.

All of the above statements agree with the findings of this investigation.

It is clear that stresses of the magnitude shown could lead to an early fatigue failure of a pipe joint submitted to repeated loading, particularly if any stress-raiser, such as a flaw in a welded joint, were present.

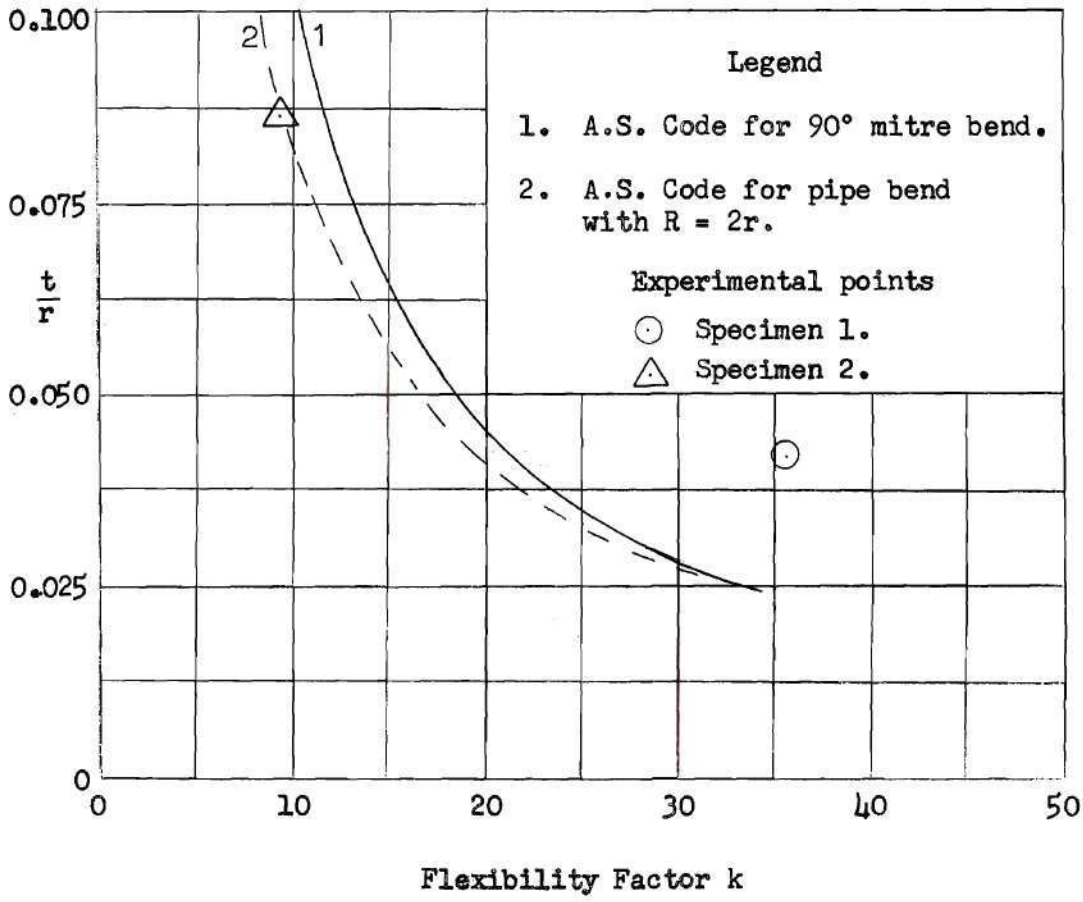

Fig. 12. Relationship between $\frac{t}{r}$ and Flexibility Factor k.

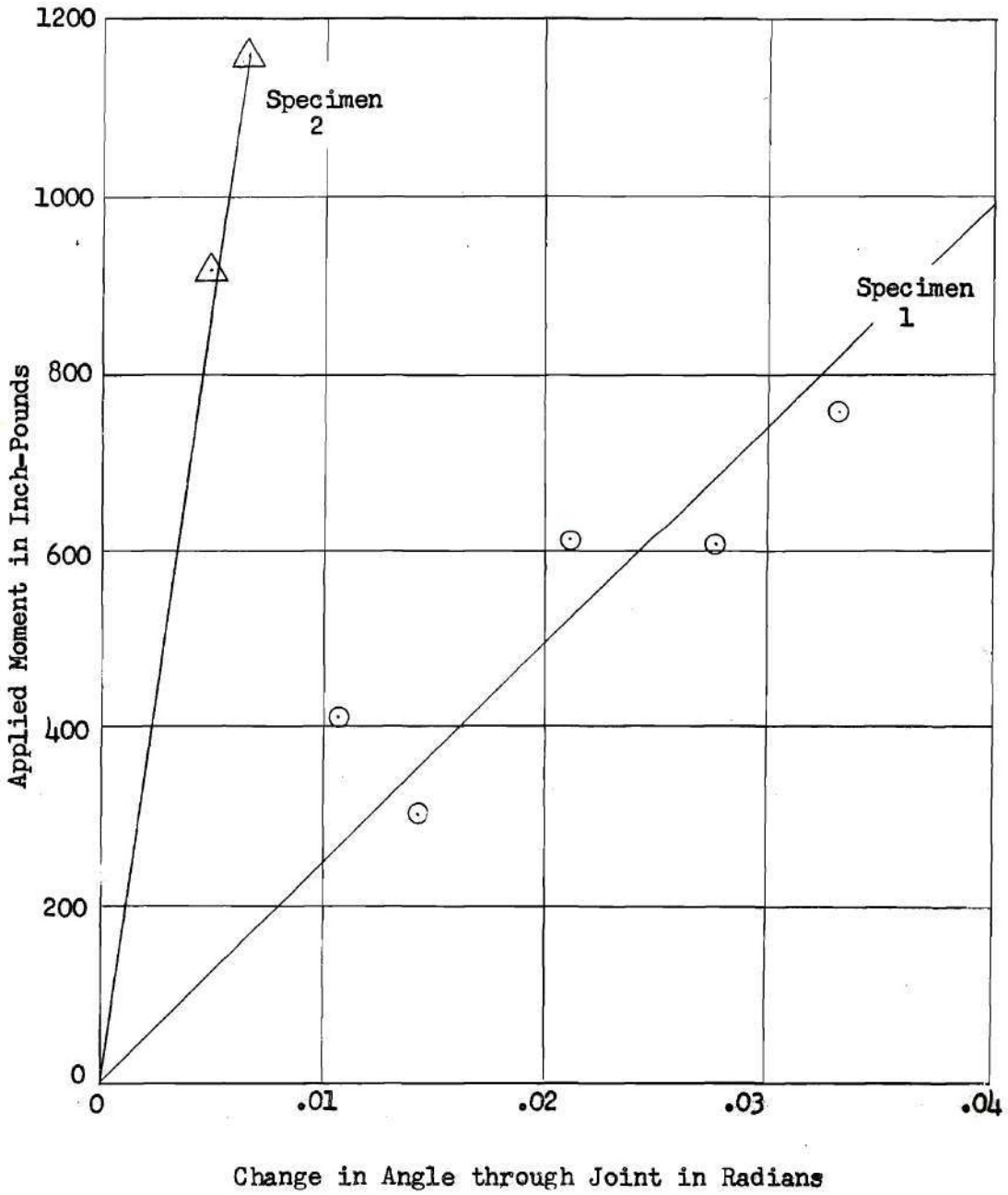

Fig. 13. Measured Joint Stiffness.

CHAPTER VI

CONCLUSIONS

The distortion of a ninety-degree pipe joint subjected to pure bending in the plane of the joint is similar to that of the radiused pipe bend. The stiffness of such a joint is much less than that which would be predicted by simple engineering theory. The Flexibility Factor for the thinner-walled of the two specimens tested was nearly twice as great as the factor obtained from the American Standard Code for Pressure Piping for a similar pipe bend of small radius or a ninety-degree mitre bend.

Local ovalization of the tubes occurs near the joint. This decreases approximately exponentially as distance from the joint increases.

A local region of very high strain exists on the centroidal axes of the tubes near the joint. The magnitude of this strain, which is parallel to the joint surface, is such that an early fatigue failure could be expected in this region with repeated loading, particularly if any stress-raiser, such as a flaw in a welded joint, were present.

APPENDIX

Test Results

TABLE 1

Deflections of Center-Line
Specimen 1

Applied Moment 416 inch-pounds (first run)

Point	Unloaded Coordinates x	y	Loaded Coordinates x	Δx	y	Δy
1	0.069	15.124	0.126	+0.057	15.146	+0.022
2	2.534	15.131	2.591	+0.057	15.144	+0.013
3	5.227	15.148	5.280	+0.053	15.148	0
4	7.694	15.146	7.748	+0.054	15.136	-0.010
5	10.223	15.159	10.290	+0.057	15.139	-0.020
6	12.698	15.182	12.754	+0.056	15.151	-0.031
7	14.874	15.141	14.932	+0.058	15.092	-0.049
				Δx - 0.057		
8	14.892	13.013	14.926	-0.023	12.960	
9	14.886	10.513	14.885	-0.058	10.461	
10	14.893	8.095	14.856	-0.094	8.047	
11	14.888	5.410	14.810	-0.135	5.363	
12	14.918	2.988	14.798	-0.177	2.940	

x values for points 8 through 12 are adjusted for translation of specimen laterally due to loading (as evidenced by x readings for points 1 through 7)

Deflections are shown in Figure 14.

Change in angle through joint = 0.01064 radians

(Continued)

TABLE 1 (Continued)

Deflections of Center-Line
Specimen 1

Applied Moment 416 inch-pounds (second run)

Point	Unloaded Coordinates x	y	Loaded Coordinates x	Δx	y	Δy
1	0.011	15.129	0.024	+0.013	15.124	-0.005
2	2.478	15.142	2.492	+0.014	15.126	-0.016
3	5.173	15.161	5.187	+0.014	15.137	-0.024
4	7.643	15.163	7.657	+0.014	15.130	-0.033
5	10.190	15.176	10.201	+0.011	15.136	-0.040
6	12.737	15.191	12.751	+0.014	15.141	-0.050
7	14.915	15.142	14.930	+0.015	15.078	-0.064
				Δx - 0.014		
8	14.927	13.014	14.922	-0.019	12.947	
9	14.913	10.514	14.875	-0.052	10.446	
10	14.913	8.097	14.839	-0.088	8.030	
11	14.899	5.414	14.788	-0.125	5.348	
12	14.920	2.990	14.773	-0.161	2.928	

Change in angle through joint = 0.01044 radians

(Continued)

TABLE 1 (Continued)

Deflections of Center-Line
Specimen 1

Applied Moment 612 inch-pounds

Point	Unloaded Coordinates x	y	Loaded Coordinates x	$\triangle x$	y	$\triangle y$
1	0.132	15.144	0.158	0.026	15.107	-0.007
2	2.598	15.117	2.625	0.027	15.099	-0.018
3	5.292	15.130	5.317	0.025	15.096	-0.034
4	7.765	15.125	7.786	0.021	15.074	-0.051
5	10.318	15.132	10.337	0.019	15.068	-0.064
6	12.857	15.136	12.877	0.020	15.051	-0.085
7	15.034	15.084	15.059	0.025	14.978	-0.106
				$\triangle x$ - 0.025		
8	15.041	12.956	15.024	-0.042	12.834	
9	15.022	10.454	14.937	-0.110	10.336	
10	15.014	8.038	14.862	-0.177	7.924	
11	14.997	5.355	14.764	-0.258	5.241	
12	15.010	2.933	14.708	-0.327	2.823	

Change in angle through joint = 0.02099 radians

(Continued)

TABLE 1 (Continued)

Deflections of Center-Line
Specimen 1

Applied Moment 306 inch-pounds

Point	Unloaded Coordinates x	y	Loaded Coordinates x	Δx	y	Δy
1	0.020	15.235	0.027	+0.007	15.225	-0.010
2	2.486	15.247	2.493	+0.007	15.233	-0.014
3	5.178	15.268	5.185	+0.007	15.248	-0.020
4	7.648	15.273	7.656	+0.008	15.243	-0.030
5	10.199	15.291	10.207	+0.008	15.253	-0.038
6	12.739	15.306	12.745	+0.006	15.258	-0.048
7	14.915	15.258	14.924	+0.009	15.190	-0.068
				Δx - 0.008		
8	14.932	13.129	14.915	-0.025	13.055	
9	14.920	10.634	14.862	-0.066	10.562	
10	14.920	8.223	14.819	-0.109	8.152	
11	14.910	5.536	14.762	-0.156	5.469	
12	14.932	3.116	14.738	-0.202	3.050	

Change in angle through joint = 0.0142 radians

(Continued)

TABLE 1 (Continued)

Deflections of Center-Line
Specimen 1

Applied Moment 612 inch-pounds

Point	Unloaded Coordinates x	y	Loaded Coordinates x	△x	y	△y
1	0.020	15.235	0.035	+0.015	15.223	-0.012
2	2.486	15.247	2.501	+0.015	15.226	-0.021
3	5.178	15.268	-	-	-	-
4	7.648	15.273	7.661	+0.013	15.225	-0.048
5	10.199	15.291	10.212	+0.013	15.230	-0.061
6	12.739	15.306	12.751	+0.012	15.225	-0.081
7	14.915	15.258	14.930	+0.015	15.145	-0.113
				△x - 0.014		
8	14.932	13.129	14.900	-0.046	-	
9	14.920	10.634	14.812	-0.122	10.511	
10	14.920	8.223	14.731	-0.203	-	
11	14.910	5.536	14.630	-0.294	5.421	
12	14.932	3.116	14.566	-0.380	3.000	

Change in angle through joint = 0.0276

(Continued)

TABLE 1 (Continued)

Deflections of Center-Line
Specimen 1

Applied Moment 766 inch-pounds

Point	Unloaded Coordinates x	y	Loaded Coordinates x	△x	y	△y
1	0.020	15.235	0.059	+0.039	15.239	+0.004
2	2.486	15.247	2.522	+0.036	15.239	-0.008
3	5.178	15.268	-	-	-	-
4	7.648	15.273	7.682	+0.034	15.236	-0.037
5	10.199	15.291	-	-	-	-
6	12.739	15.306	12.773	+0.034	15.231	-0.075
7	14.915	15.258	14.952	+0.037	15.146	-0.112
				△x - 0.036		
8	14.932	13.129	14.916	-0.052	13.012	
9	14.920	10.634	14.814	-0.132	-	
10	14.920	8.223	14.720	-0.236	8.105	
11	14.910	5.536	14.605	-0.341	-	
12	14.932	3.116	14.527	-0.441	3.008	

Change in angle through joint = 0.0331 radians

TABLE 2

Deflections of Center-Line
Specimen 2

Applied Moment 920 inch-pounds

Point	Unloaded Coordinates x	y	Loaded Coordinates x	△x	y	△y
1	0.982	15.074	1.005	+0.023	15.065	-0.009
2	4.492	15.103	4.516	+0.024	15.094	-0.009
3	7.415	15.202	7.439	+0.024	15.182	-0.020
4	10.269	15.239	10.292	+0.023	15.209	-0.030
5	13.528	15.310	13.550	+0.022	15.268	-0.042
6	16.105	15.364	16.127	+0.022	15.312	-0.052
				△x - 0.022		
7	16.525	14.763	16.544	-0.003	14.705	
8	16.522	12.227	16.522	-0.022	12.168	
9	16.516	9.766	16.487	-0.051	9.706	
10	16.489	6.728	16.444	-0.067	6.719	
11	16.499	3.712	16.425	-0.096	3.654	
12	16.485	1.269	16.389	-0.118	1.213	

Change in angle through joint = 0.0049 radians

(Continued)

TABLE 2 (Continued)

Deflections of Center-Line
Specimen 2

Applied Moment 1164 inch-pounds

Point	Unloaded Coordinates x	y	Loaded Coordinates x	$\triangle x$	y	$\triangle y$
1	0.982	15.074	-0.215	-1.197	15.066	-0.008
2	4.492	15.103	3.296	-1.196	15.094	-0.009
3	7.415	15.202	6.216	-1.199	15.178	-0.024
4	10.269	15.239	9.071	-1.198	15.205	-0.034
5	13.528	15.310	12.330	-1.198	15.262	-0.048
6	16.105	15.364	14.906	-1.199	15.301	-0.063
				$\triangle x + 1.198$		
7	16.525	14.763	15.324	-0.003	14.688	
8	16.522	12.227	15.298	-0.026	12.157	
9	16.516	9.766	15.264	-0.054	9.692	
10	16.489	6.728	15.205	-0.086	6.709	
11	16.499	3.712	15.180	-0.121	3.647	
12	16.485	1.269	15.136	-0.151	1.205	

Change in angle through joint = 0.00678 radians

TABLE 3

Measured Tube Diameters
Specimen 1

Diameters in Loading Plane				Diameters Normal to Loading Plane		
Distance from outer corner	Unloaded Diameter	Moment 416 inch-pounds		Unloaded Diameter	Moment 416 inch-pounds	
		Diam.	Change in Diam.		Diam.	Change in Diam.
			Horizontal Tube			
4.0	-	-	-	6.087	6.191	+0.104
6.5	6.085	6.017	-0.068	6.085	6.167	+0.082
9.0	6.084	6.028	-0.056	6.083	6.143	+0.062
11.5	6.083	6.040	-0.043	6.085	6.128	+0.043
14.0	6.080	6.049	-0.031	6.089	6.119	+0.030
16.5	6.077	6.056	-0.021	6.093	6.116	+0.023
			Vertical Tube			
4.0	-	-	-	6.083	6.188	+0.105
6.5	6.079	6.016	-0.063	6.085	6.158	+0.073
9.0	6.077	6.035	-0.042	6.086	6.136	+0.050
11.5	6.076	6.056	-0.020	-	-	-

(Continued)

TABLE 3 (Continued)

Measured Tube Diameters
Specimen 1

Diameters in Loading Plane				Diameters Normal to Loading Plane		
Distance from outer corner	Unloaded Diameter	Moment 612 inch-pounds		Unloaded Diameter	Moment 612 inch-pounds	
		Diam.	Change in Diam.		Diam.	Change in Diam.
			Horizontal Tube			
4.0	-	-	-	6.093	6.252	+0.159
6.5	6.079	5.978	-0.101	6.094	6.213	+0.119
9.0	6.077	5.998	-0.079	6.087	6.175	+0.088
11.5	6.077	6.016	-0.061	6.087	6.152	+0.065
14.0	6.076	6.031	-0.045	6.090	6.137	+0.047
16.5	6.073	6.038	-0.035	6.095	6.131	+0.036
			Vertical Tube			
4.0	-	-	-	6.090	6.253	+0.163
6.5	6.077	5.975	-0.102	6.090	6.204	+0.114
9.0	6.077	6.003	-0.074	-	-	-
11.5	6.077	6.028	-0.049	-	-	-
14.0	6.077	6.064	-0.013	-	-	-

TABLE 4

Measured Tube Diameters
Specimen 2

Diameters in Loading Plane				Diameters Normal to Loading Plane		
Distance from outer corner	Unloaded Diameters	Moment 416 inch-pounds		Unloaded Diameter	Moment 416 inch-pounds	
		Diam.	Change in Diam.		Diam.	Change in Diam.
			Horizontal Tube			
6.5	6.101	6.088	-0.013	6.098	6.117	+0.019
9.0	6.101	6.091	-0.010	6.098	6.108	+0.010
11.5	6.101	6.096	-0.005	6.098	6.106	+0.008
14.0	6.101	6.098	-0.003	6.100	6.105	+0.005
16.5	6.101	6.098	-0.003	6.102	6.105	+0.003
			Vertical Tube			
6.5	6.095	6.082	-0.013	6.101	6.117	+0.016
9.0	6.096	6.089	-0.007	6.100	6.108	+0.008
11.5	6.099	6.095	-0.004	-	-	-
14.0	6.099	6.100	+0.001	-	-	-

(Continued)

TABLE 4 (Continued)

Measured Tube Diameters
Specimen 2

Diameters in Loading Plane				Diameters Normal to Loading Plane		
Distance from outer corner	Unloaded Diameter	Moment 920 inch-pounds		Unloaded Diameter	Moment 920 inch-pounds	
		Diam.	Change in Diam.		Diam.	Change in Diam.
		Horizontal Tube				
6.5	6.101	6.071	-0.030	6.098	6.130	+0.032
9.0	6.101	6.082	-0.019	6.098	6.118	+0.020
11.5	6.101	6.090	-0.011	6.098	6.112	+0.014
14.0	6.101	6.094	-0.007	6.100	6.108	+0.008
16.5	6.101	6.091	-0.010	6.102	6.104	+0.002
		Vertical Tube				
6.5	6.095	6.066	-0.029	6.101	6.132	+0.031
9.0	6.096	6.080	-0.016	6.100	6.116	+0.016
11.5	6.099	6.092	-0.007	-	-	-
14.0	6.099	6.100	+0.001	-	-	-

(Continued)

TABLE 4 (Continued)

Measured Tube Diameters
Specimen 2

Distance from outer corner	Diameters in Loading Plane			Diameters Normal to Loading Plane		
	Unloaded Diameter	Moment 1164 inch-pounds		Unloaded Diameter	Moment 1164 inch-pounds	
		Diam.	Change in Diam.		Diam.	Change in Diam.
			Horizontal Tube			
4.0	-	-	-	-	6.145	+0.045
6.5	6.102	6.068	-0.034	6.100	6.134	+0.034
9.0	6.102	6.079	-0.023	6.101	6.122	+0.021
11.5	6.103	6.089	-0.014	6.103	6.114	+0.011
14.0	6.102	6.094	-0.008	6.103	6.110	+0.007
16.5	6.101	6.095	-0.006	6.105	6.111	+0.006
			Vertical Tube			
4.0	-	-	-	6.104	6.151	+0.047
6.5	6.095	6.062	-0.033	6.103	6.138	+0.035
9.0	6.096	6.078	-0.018	-	-	-
11.5	6.099	6.096	-0.003	-	-	-

TABLE 5

Strain Gage Locations

Gage	Type	Resistance ohms	Gage Factor	Gage Length	Location X	Location Y	Type of Gage
1	A5-1	119.6	1.98	1/2	1.15	-	Two axials to form a T
2					1.78	-	
3	A5-1	120.4	2.00	1/2	4.0	-	Axial
4	A5-1	119.6	1.98	1/2	7.1	-	Axial
5	A7	120	1.98	1/4	3.9	-	Three axials to form 90° rosette
6					3.9	0.3	
7					4.1	0.3	
8	A5-1	120.4	1.98	1/2	7.25	-0.4	Three axials to form 90° rosette
9					6.6	-	
10					6.6	0.4	
11	A5-1	120.4	2.00	1/2	7.1	-	Two axials to form a T
12					7.75	-	
13	AX5	120	2.00	15/32	7.71	-	" " "
14					7.75	-	

(Continued)

TABLE 5 (Continued)

Strain Gage Locations

Gage	Type	Resistance ohms	Gage Factor	Gage Length	Location X	Location Y	Type of Gage
15	AX5	120	2.00	15/32	1.15	-	
16					1.15	-	
17	A5-1	120.4	1.98	1/2	7.1	-	Axial
18	A7	120	1.98	1/4	3.9	-	Three axials to form 90° rosette
19					3.9	0.3	
20					4.1	0.3	
21	AD7	120	1.95	1/4	6.6	-	Three axials to form 90° rosette
22					6.6	0.4	
23					7.25	-0.4	

For dimensions X and Y see Fig. 8.

TABLE 6

Strain Gage Readings
Specimen 1

Gage	Cable Load (Pounds)										
	100	100	100	100	50	75	100	100	125	*Average	Corrected for Gage Factor
1	-490	-460			-280	-415	-495	-500	-560	-486	-491
2	135	135			+ 85	+125	+150	+150	+170	+144	+145
3			-755	-815	-355	-740	-875	-875	-980	-828	-828
4			-1200	-1290	-580	-1170	-1390	-1375	-1530	-1310	-1323
5	+2165	+2030			+990	+2030	+2460	+2405	+2735	+2280	+2303
6	+1155	+1000			+580	+1180	+1450	+1365	+1535	+1267	+1280
7	+3235	+3080			+1330	+2800	+3380	+3400	+3940	+3260	+3293
8	+2080	+1960	+1805	+1930	+915	+1790	+2110	+2110	+2380	+1995	+2015
9	-575	-570	-490	-575	-215	-445	-510	-545	-610	-534	-539
10	+550	+520	+485	+495	+260	+495	+590	+590	+670	+546	+551
11	-905	-860			-390	-790	-950	-940	-1055	-904	-904
12	-60	-50								-55	-55

(Continued)

TABLE 6 (Continued)

Strain Gage Readings
Specimen 1

Gage	Cable Load (Pounds)										
	100	100	100	100	50	75	100	100	125	*Average	Corrected for Gage Factor
13	+680	+650			+325	+600	+720	+720	+805	+689	+689
14	-140	-130			-45	-110	-140	-135	-145	-130	-130
15	Gages shorted out inside gage										
16	Gages shorted out inside gage										
17	+1350	+1280			+620	+1190	+1405	+1390	+1550	+1345	+1358
18	-855	-820			-345	-730	-880	-890	-1015	-853	-862
19	-275	-265			-85	-210	-260	-265	-320	-261	-264
20	-5265	-5000			-2230	-4580	-5460	-5470	-6190	-5250	-5302
21			-180	-240	-70	-165	-210	-215	-240	-205	-210
22			-1285	-1430	-620	-1260	-1530	-1530	-1720	-1440	-1477
23			-1265	-1320	-640	-1310	-1560	-1540	-1720	-1410	-1447

*Averages obtained by method of least squares for a cable load of 100 pounds

TABLE 7

Stress Values from Averaged Strain Gage Readings
for Moment of 612.5 inch-pounds

Specimen 1

Gages	Strain	Stress
1,2 (at location of Gage 2)	$\epsilon_1 = -550$	$\sigma_1 = -227$
	$\epsilon_2 = +145$	$\sigma_2 = -22$
11,12	$\epsilon_{11} = -904$	$\sigma_{11} = -420$
	$\epsilon_{12} = -55$	$\sigma_{12} = -170$
13,14	$\epsilon_{13} = +689$	$\sigma_{13} = +293$
	$\epsilon_{14} = -130$	$\sigma_{14} = +51$
5,6,7	$\epsilon_5 = +2303$	$\sigma_u = +2190$
	$\epsilon_6 = +1280$	$\sigma_v = +1250$
	$\epsilon_7 = +3293$	
	$\epsilon_u = +4388$	
	$\epsilon_v = +1208$	
	$\theta = 54°$	
18,19,20	$\epsilon_{18} = -862$	$\sigma_u = -2960$
	$\epsilon_{19} = -264$	$\sigma_v = -833$
	$\epsilon_{20} = -5302$	
	$\epsilon_u = -6672$	
	$\epsilon_v = +508$	
	$\theta = 64°$	

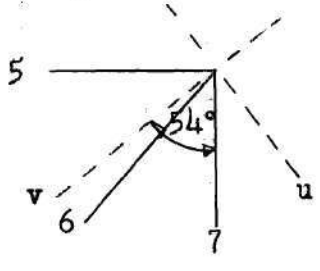

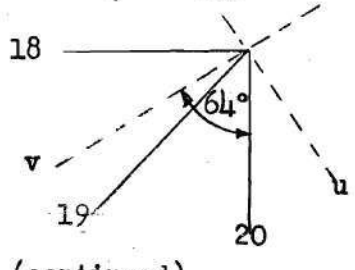

(continued)

TABLE 7 (Continued)

Stress Values from Averaged Strain Gage Readings
for Moment of 612.5 inch-pounds

Specimen 1

Gages	Strain	Stress
8,9,10	$\epsilon_8 = +2015$ $\epsilon_9 = -539$ $\epsilon_{10} = +551$ $\epsilon_u = +2028$ $\epsilon_v = -552$ $\theta = 4°$	$\sigma_u = +836$ $\sigma_v = +72$ 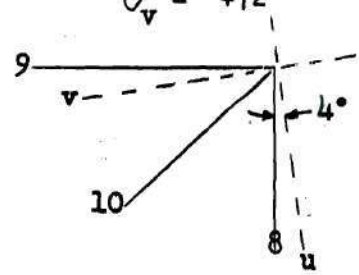
21,22,23	$\epsilon_{21} = -210$ $\epsilon_{22} = -1477$ $\theta_{23} = -1447$ $\epsilon_u = +68$ $\epsilon_v = +1725$ $\theta = 23°$	$_u = -244$ $_v = -775$ 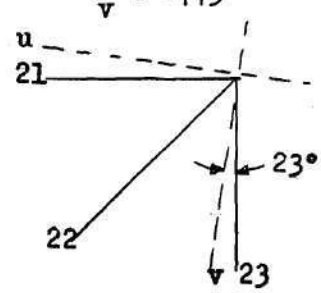

Strains in micro-inches per inch

Stresses in pounds per square inch

E = 400,000 pounds per square inch $\mu = 0.35$

See Fig. 8. for gage locations

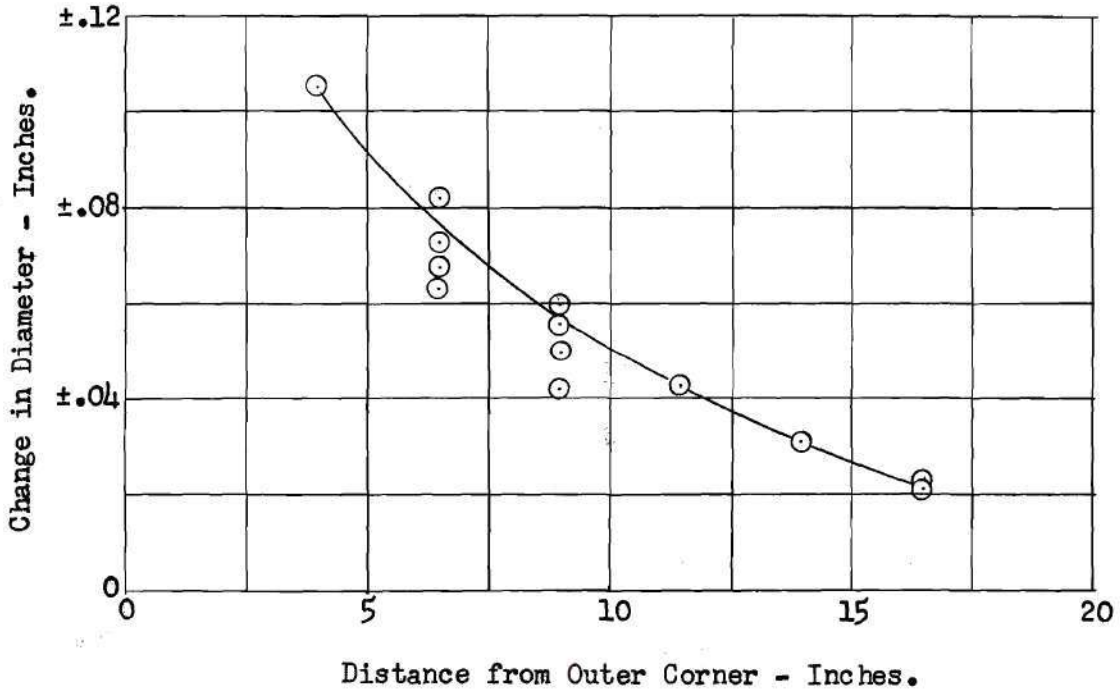

Fig. 14. Change in Diameter - Specimen 1.

416 inch-pound moment.

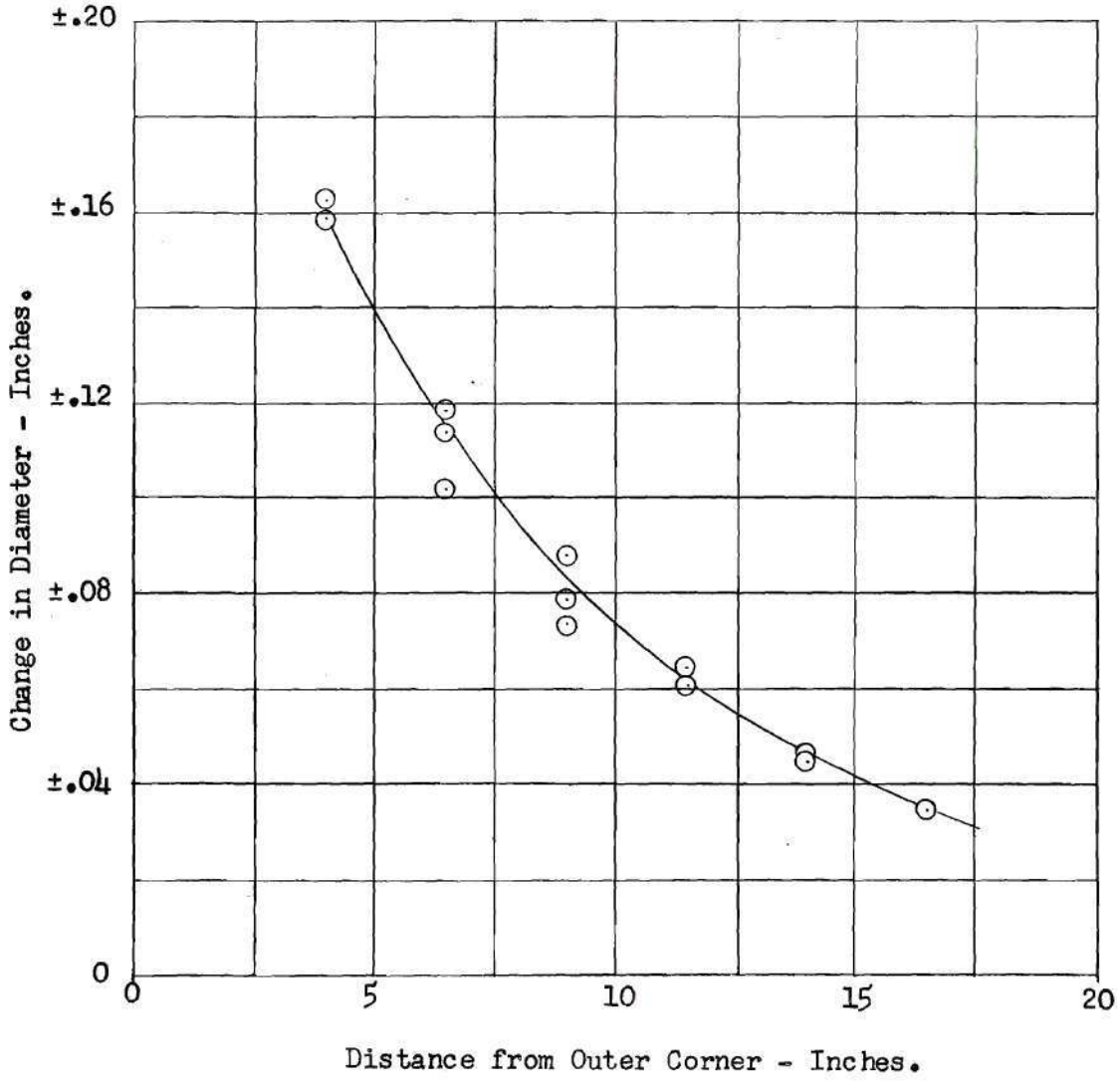

Fig. 15. Change in Diameter - Specimen 1.

612 inch-pound moment.

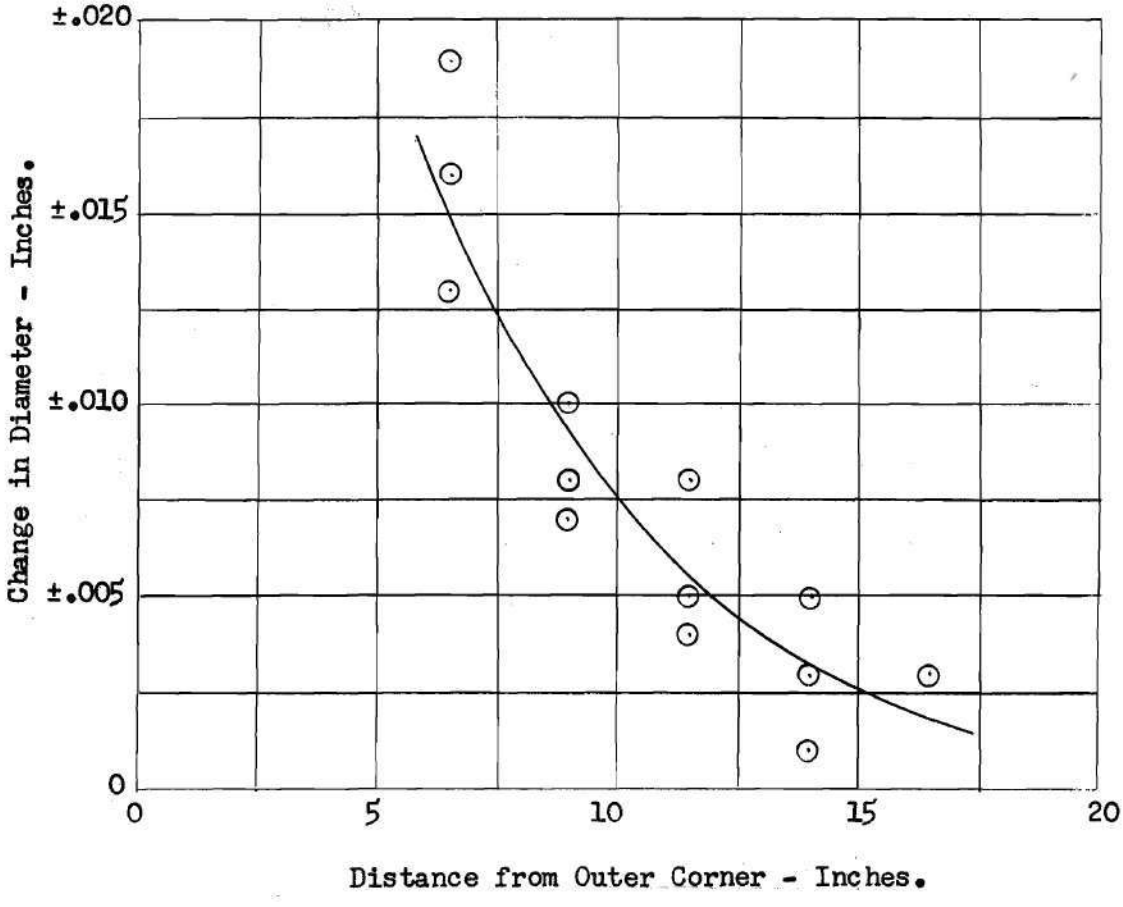

Fig. 16. Change in Diameter - Specimen 2.

416 inch-pound moment.

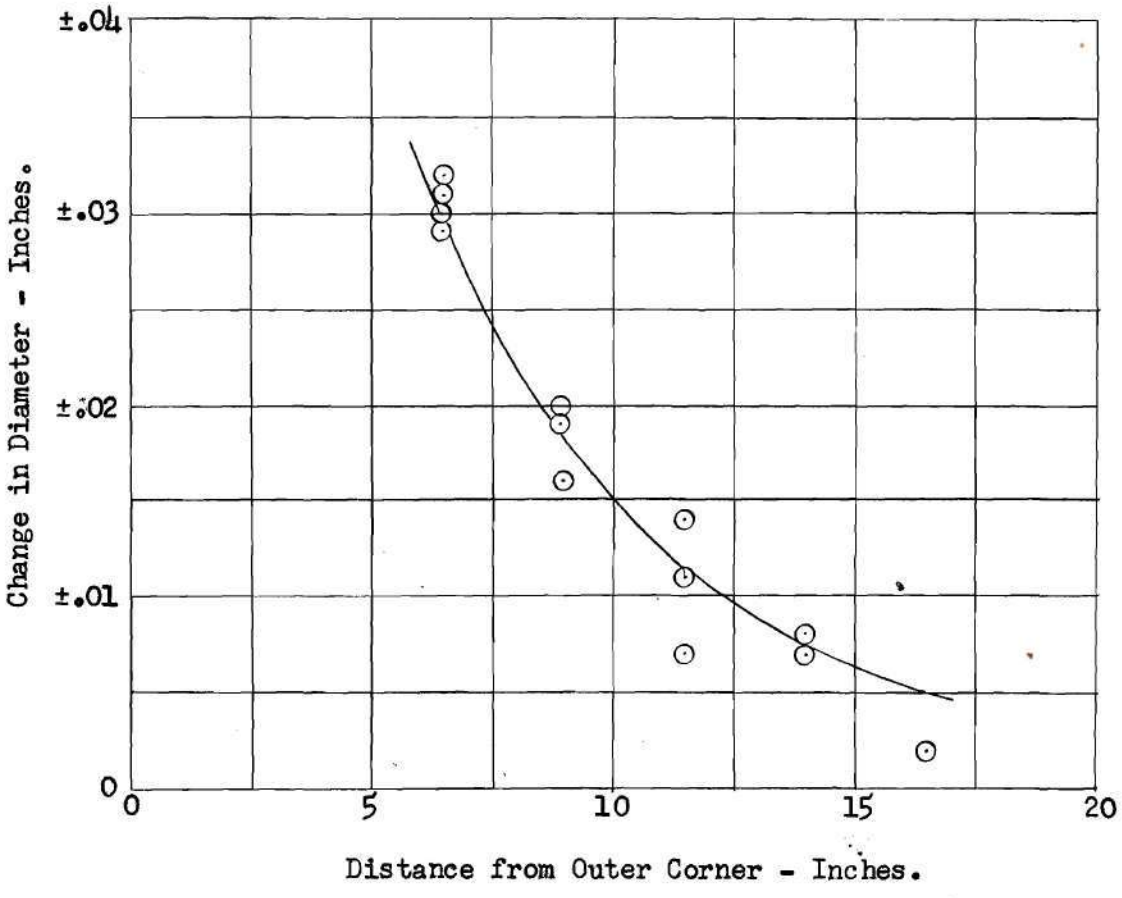

Fig. 17. Change in Diameter - Specimen 2.
920 inch-pound moment.

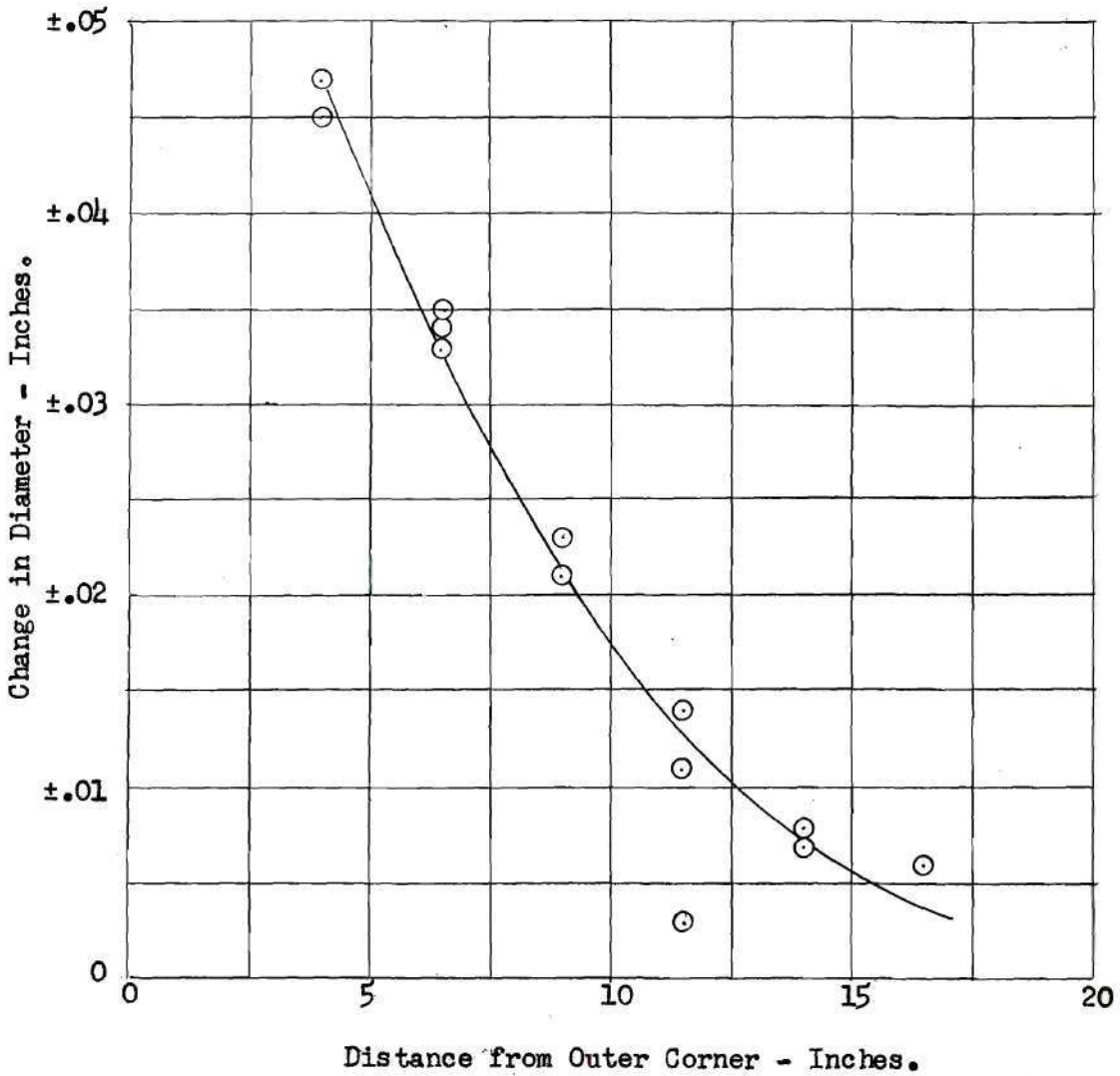

Fig. 18. Change in Diameter - Specimen 2.
1164 inch-pound moment.

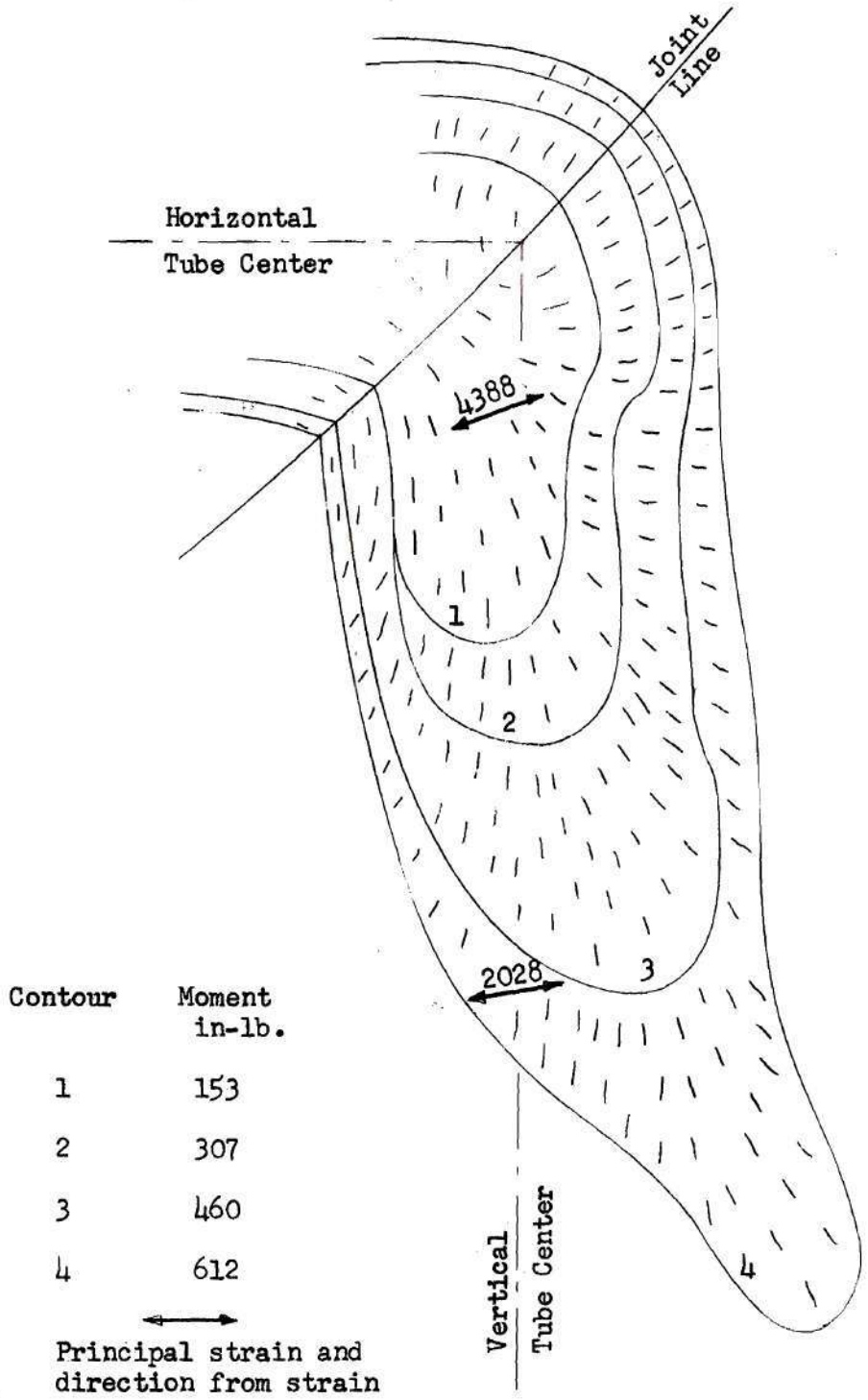

Fig. 19. Stresscoat Pattern.

BIBLIOGRAPHY

1. Karman, Th. von, "Über die Formänderung dünnwandiger Rohre," Zeitschrift des Vereines deutscher Ingenieure, Vol. 55(1911), p. 1889.

2. Gross, N., "Experiments on Short-Radius Pipe Bends," Proceedings of the Institution of Mechanical Engineers, London. Vol. 1B(1952-53), p. 465.

3. American Society of Mechanical Engineers, American Standard Code for Pressure Piping, A.S.A. B31.1(1955), p. 92.

4. Den Hartog, J. P., Advanced Strength of Materials, 1st ed., McGraw-Hill Book Company, Inc., 1952, pp. 234-245.

5. Magnaflux Corporation, Chicago 31, Illinois. Principles of Stresscoat, (1955).

6. Rohm and Haas Company, Philadelphia 5, Pennsylvania, Plexiglas Handbook for Aircraft Engineers (1951), p. 4.

7. Markl, A. R. C., "Piping Flexibility Analysis," Transactions of the American Society of Mechanical Engineers, Vol. 77, Feb. 1955, p. 129.

8. Rodabaugh, E. C., and George, H. H., "Effect of Internal Pressure on the Flexibility and Stress-Intensification Factors of Curved Pipe or Welding Elbows," Transactions of the American Society of Mechanical Engineers, Vol. 79, May 1957, p. 940.

9. Markl, A. R. C., "Fatigue Tests of Welding Elbows and Comparable Double-Mitre Bends," Transactions of the American Society of Mechanical Engineers, Vol. 69, 1947, p. 879.

10. Gross, N., Experiments on Short-Radius Pipe Bends," Proceedings of the Institution of Mechanical Engineers, Vol. 79, May 1957, p. 473.

11. Markl, A. R. C., "Fatigue Tests of Welding Elbows and Comparable Double-Mitre Bends," Transactions of the American Society of Mechanical Engineers, Vol. 79, May 1957, p. 875.

12. Pardue, T. S., and Vigness, I., "Properties of Thin-Walled Curved Tubes of Short Bend Radius," Transactions of the American Society of Mechanical Engineers, Vol. 73, 1951, p. 77.